

REVIEW ARTICLE

Radionuclide Liver Imaging: Is there a role?

Ali Nawaz Khan[1,*], Ghulam Mustafa Shah Syed[2], Durr-e-Sabih[3], Qaisar Hussain Siraj[4]

[1]Department of Radiology, North Manchester General Hospital, Pennine Acute Hospital Trust, Manchester,
[2]Nuclear Medicine Section, Department of Radiology, King Fahad Medical City, Riyadh, Saudi Arabia
[3]Multan Institute of Nuclear Medicine & Radiotherapy (MINAR)
[4]Nuclear Medicine Department, Farwania Hospital Kuwait

Abstract Hepatic scintigraphy has had to take a back seat for the past 2 decades because of continuing development of anatomical imaging. Ultrasound, CT, and MRI have more or less replaced Tc-99m colloid liver-spleen scan (SCS). However, the standard SCS survives and has an important role in certain niche areas where it makes a significant clinical contribution. The standard SCS gave relatively non-specific results. Now, we are moving to more tissue-specific scintigraphic scanning e.g., somatostatin imaging. Positron Emission Tomography (PET) continues to evolve as in other areas of Nuclear Imaging. Hepatobiliary scanning with iminodiacetic acid (IDA) compounds continue to play a prominent role in certain areas. Recent developments have concentrated on new equipment and increased availability of new radionuclides. These are the subject of this review. This review also describes the value of physiological liver scintigraphy, including gallium scanning as well as dynamic flow imaging of the liver such as hepatic artery perfusion scintigraphy and tagged red cell scintigraphy.

Key words: *Radionuclide liver imaging, SPET-CT, Hepatobiliary imgaing, Gallium-67 scanning*

***Correspondence**

Prof Ali Nawaz Khan
North Manchester General Hospital
Pennine Acute Hospital Trust
Manchester M8 5RB
Email: drkhan1966@msn.com

Introduction

Despite Nuclear Medicine (NM) losing ground to anatomical imaging, NM has re-packaged itself effectively into offering more functional and tissue-specific liver imaging. Many useful indications for the SCS imaging remains and have acquired even a more significant role complimenting anatomical imaging [1-18]. SCS imaging of splenic tissue complements with denatured radiolabelled red blood cells scanning [3 & 11]. A combination of SCS and hepatobiliary scintigraphy (HIDA) may predict response to interferon in the treatment of chronic hepatitis [2]. Laparoscopic excision of retained splenic tissue for recurrent haematologic disease after conventional splenectomy is aided by intraoperative gamma probe localization using SCS [17 &18]. NM continues to play a decisive role in the diagnosis of a hepatic haemangioma, benign solid liver tumours including hepatic adenoma and focal fatty infiltration of the

 2221-0288(201401/01)4:1<01:RLIITA>2.0.TX;2-M

liver. Further inroads are in characterising liver metastases, hepatoblastoma and molecular imaging of HCC [19-26]. somatostatin receptor scintigraphy has an essential role in characterising neuro endocrine (NET) and gastroenteropancreatic tumours and targeted therapy [27-31].

Today, HIDA is used in a clinical setting, which is very different from its use in the diagnoses of acute cholecystitis and biliary atresia [32-41]. Acute acalculous cholecystitis (AAC) is a difficult diagnosis because of the complex clinical setting in which the entity develops. Ultrasound (often sequential) and HIDA scans are the most reliable diagnostic modalities here [32].

Radiofrequency ablation (RFA) is one of the alternatives in the management of liver tumours, especially in patients who are not candidates for surgery. The success of RFA depends on creating adequate volumes of tissue destruction with adequate "clear margin," with improved delivery of RFA. Follow-up imaging is the key to the degree of coagulation necrosis achieved. Contrast-enhanced CT, MRI, ultrasound or PET, are applied to control the effectiveness of RFA [42].

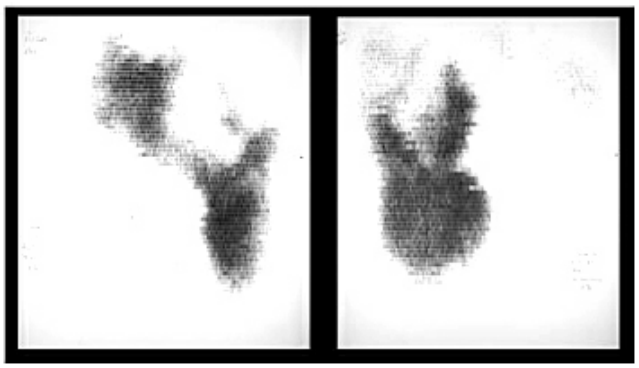

Figure 1 *Colloid liver scan obtained with a rectilinear scanner in the anterior ((right) and right lateral (left) projections. Note: we have come a long way since the days of a rectilinear scanner, which despite a very slow process and very larges sized pixels was the only technique available for the diagnosis of a lesion within the liver.*

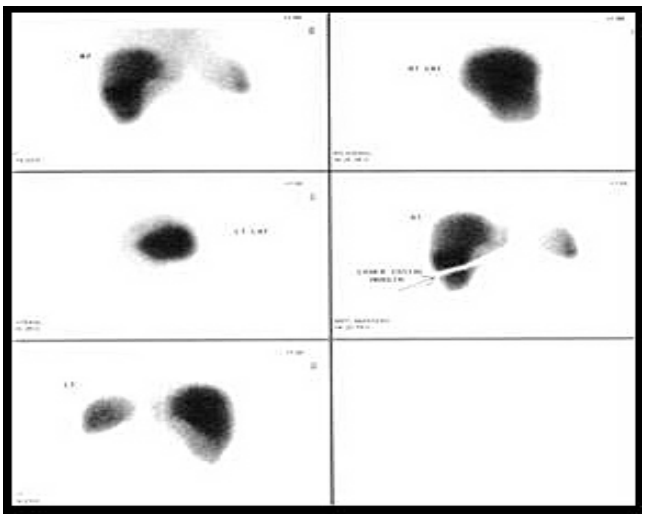

Figure 2 *The advent of a gamma camera was a great advance and colloid scan remained the only modality available for liver lesions for quite some time.*

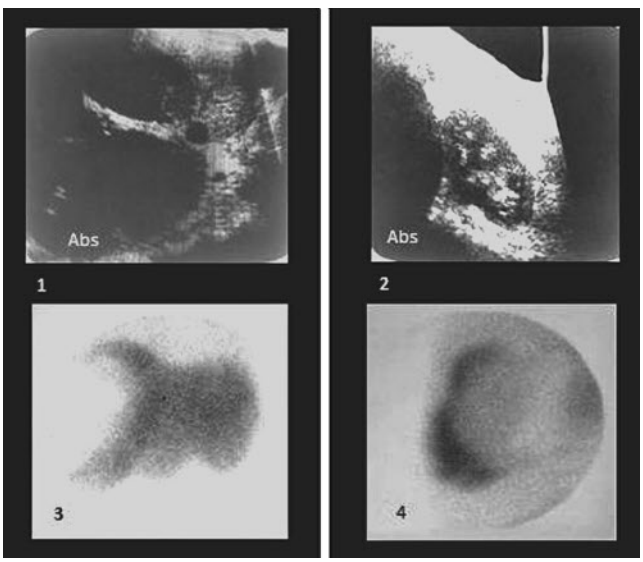

Figure 3 *Historical images from the late seventies of patient with a history of foreign travel who presented to our Infection Unit with fever, right upper quadrant pain and jaundice. Image 1 & 2 were the first ultrasound images produced in our department using a bistable B scanner that was recently upgraded to a gray scale machine. The images show a large abscess (Abs) but our ID physicians could only trust a colloid scan! The colloid images show a large space-occupying lesion within the liver, proved amoebic abscess.*

In the last two decades, impressive strides have been made in liver surgery, but survival is dependent on a number of prognostic indicators. Some indicators are haematological/bochemical whilst others are based on imaging. NM plays a pivotal role in establishing the presence of hepatopulmonary syndrome and intrapulmonary shunts [43-55].

Continuing role of SCS in characterizing splenic tissue

Many useful indications for the SCS imaging remains and have acquired even a more significant role complimenting anatomical imaging (1-18). See Figures 1- 14.

Splenunculi are small nodules of splenic tissue that are detached from the rest of the spleen. Splenunculi are common, seen in up to 16% of CTs of the abdomen and up to 30% of autopsies. They are benign and asymptomatic. Splenunculi need distinguishing from pathological lymph nodes in cancer staging. Splenunculi can be evaluated with Tc-99m labelled sulphur colloid SPECT imaging [4-5].

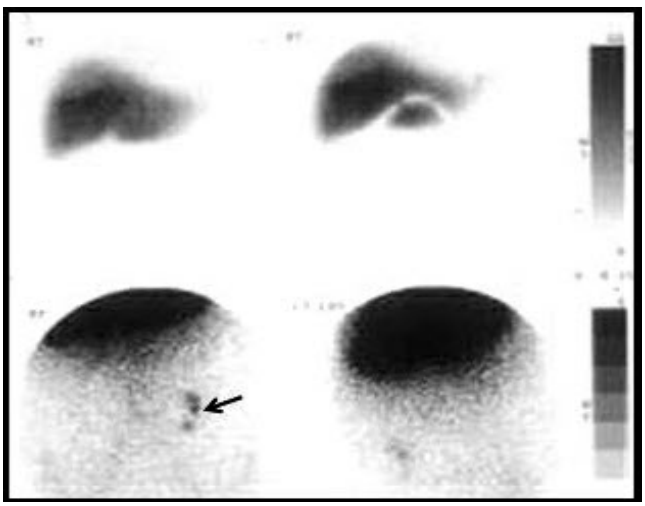

Figure 4 *Colloid scan shows uptake in omental splenic implants following splenectomy for splenic rupture. After splenectomy, a portion of spleen is implanted in the omentum to carry on some of the functions of spleen, such as immunological function. The omental implant can be seen as focal area of uptake on a sulphur colloid scan (arrow).*

Splenectomy is used to treat immune thrombocytopenic purpura. However, the disease may relapse despite splenectomy. A leading cause is the presence of an accessory spleen, which may become enlarged significantly with underlying pathologies such as presence of portal hypertension. The presence of an ectopic spleen should be borne in mind in patients diagnosed with immune thrombocytopenic purpura with relapsing hypersplenism following splenectomy. On anatomical imaging, an accessory spleen may be confused with other masses. Colloid or denatured RBC scan offers a specific diagnosis. See Figure 5.

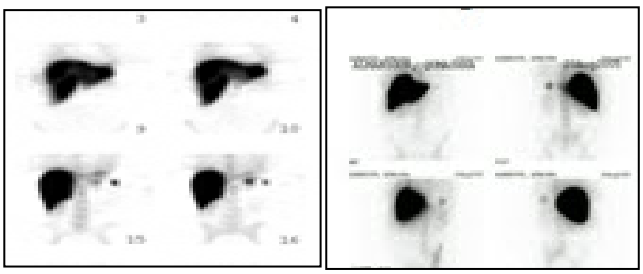

Figure 5 *The post splenectomy colloid planar images show two splenules (right) and dynamic planar/SPECT colloid images show a post splenectomy accessory spleen (left).*

Accessory spleens occur in 10% to 15% of the population. In 1% to 2%, they are located in the pancreatic tail [6]. Ectopic spleens may mimic peri-pancreatic/pancreatic tumours. Intra-pancreatic ectopic splenic tissue is rarely detected owing to its asymptomatic nature but is detected incidentally on US, CT or MRI. One such asymptomatic case has been where a CT scan revealed a 1.5 cm mass in the distal pancreas [7]. The tumour markers "CA 19-9 and CEA" were slightly raised, and a pancreatic neoplasm was suspected. At surgery, an accessory spleen within the pancreatic tail was confirmed. The clinical significance of intrapancreatic accessory spleens resides in the imitation of pancreatic cancer. An Octreotide scan, SCS and heat-damaged red blood cells should be undertaken to distinguish these lesions from NET, hypervascular metastases and pancreatic carcinoma even if super

paramagnetic iron oxide MRI contrast agent may be used in the future [8]. If the tests are equivocal, diagnostic laparotomy or laparoscopy is recommended. Despite the impressive strides in imaging techniques, a definitive diagnosis of cystic lesions in the pancreas remains elusive. An epithelial splenic cyst in an intrapancreatic accessory spleen has been reported in a 26-year-man old female. The patient who had no clinical manifestations presented with a cyst in the tail of the pancreas diagnosed by ultrasonography. A spleen-preserving distal pancreatectomy was performed with the presumptive diagnosis of a mucinous cystic tumour originating from the pancreas. The pathological examination revealed the cyst to be stratified squamous epithelium, surrounded by splenic tissue and the final diagnosis was epithelial splenic cyst in an intrapancreatic accessory spleen [9].

Ectopic splenic tissue within the stomach wall may mimic intramural tumour by endoscopy, endoscopic ultrasonography and CT. Technetium-99m sulphur colloid scintigraphy may reveal the true nature of the mass [15].

Ectopic splenic tissue can be identified by Tc-colloid scan within the thorax. A case report describes a highly unusual finding of ectopic splenic tissue in both the thoracic and abdominal cavities in a patient with recurrent ITP [12].

Stein *et al.* report a pre-transplant patient who was found to have several soft-tissue abdominal masses on MRI. The patient gave an account of splenectomy following a traumatic rupture of his spleen at the age of 12 years. His clinical background was pertinent for a traumatic rupture of the spleen at the age of 12 years, for which he required a splenectomy. He had no symptoms or physical findings to suggest a lympho proliferative disease or other malignant process. His peripheral blood smear was remarkable for the absence of Howell-Jolly bodies. The Tc-99m-sulphur colloid liver-spleen scan confirms the presence of splenosis presenting as abdominal masses on CT, MRI or US especially in patients with a history of

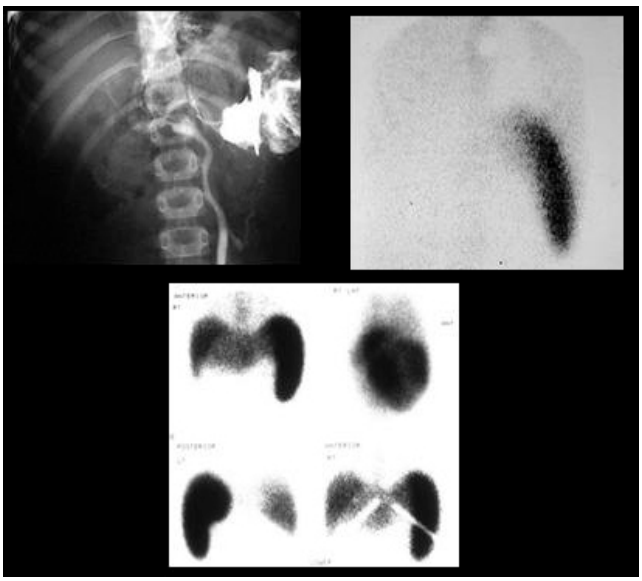

Figure 6 *Splenomegaly from a variety of causes shown on colloid scans*

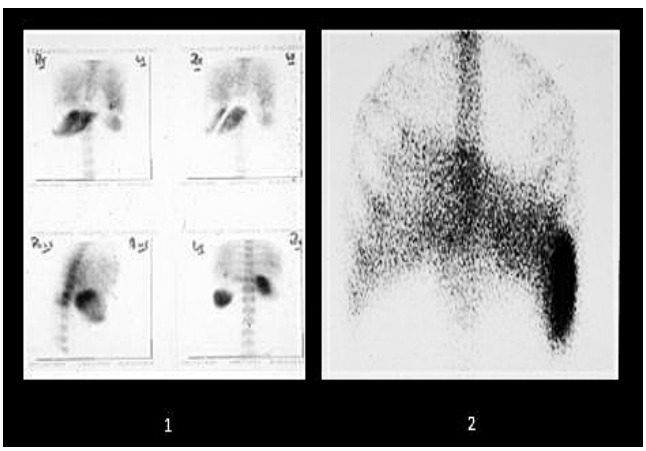

Figure 7 *In ^{99m}Tc sulphur colloid scan, a colloid shift refers to the abnormal bio distribution of radiotracer. Many causes of colloid shift exist the most common are hepatic cirrhosis, diffuse hepatic metastases, diabetes, and blunt trauma to the spleen. ^{99m}Tc sulphur colloid scintig raphy can be used in differentiating non-cirrhotic portal fibrosis from liver cirrhosis. Image 1 is from severely diabetic patient (note lack of splenomegaly) and Image 2 from a patient with cirrhosis (note the presence of splenomegaly)*

traumatic splenic rupture as a child [13].

Enlargement of accessory spleen following splenectomy may mimic an adrenal tumour. A radionuclide imaging with technetium sulphur colloid can confirm the presence of splenic tissue and help avoid more invasive procedures [14].

Ota and associates encountered a case of splenic pseudotumour. It contained cystic and solid components and a higher vascularity than the proper spleen on dynamic CT. An accessory spleen was considered most likely, but the differential diagnosis still included malignant lymphoma and metastatic tumour. The diagnosis was obtained by technetium-99m Sn colloid scintigraphy [16].

Denatured radiolabelled red blood cells may complement SCS characterization of splenic tissue [3 & 11].

Tc sulphur colloid and denatured red blood scans are used to evaluate patients in idiopathic thrombocytopenic purpura for residual splenic tissue following splenectomy. A positive technetium-labelled heat-damaged red blood cell imaging has been described in a patient with a negative colloid scan. This report emphasizes the value of the denatured red blood cells in the backdrop of strong clinical suspicion for residual splenic tissue following a negatives sulfur colloid study [3].

A combination of SCS and hepatobiliary scintigraphy (HIDA) may predict response to interferon in the treatment of chronic hepatitis [2]. Laparoscopic excision of retained splenic tissue for recurrent haematologic disease after conventional splenectomy is aided by intraoperative gamma probe localization using SCS. However, intraoperative identification of residual splenic tissue remains [17-18].

Following, splenectomy the liver may undergo remodelling with hypertrophy of the left lobe, which may mimic hypertrophy of an accessory spleen on sulphur colloid scans. This is a situation where a false-positive test may occur in a post-splenectomy case of possible splenic simulation in suspected of hypersplenism [10].

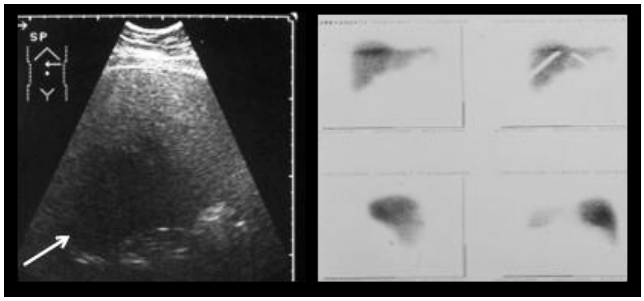

Figure 8 *^{133}Xe and ^{99m}Tc colloidal SPECT studies can reliably characterise focal fatty sparing and focal fatty infiltration. This case shows characterisation of focal fatty sparing on planar ^{99m}Tc colloidal imaging*

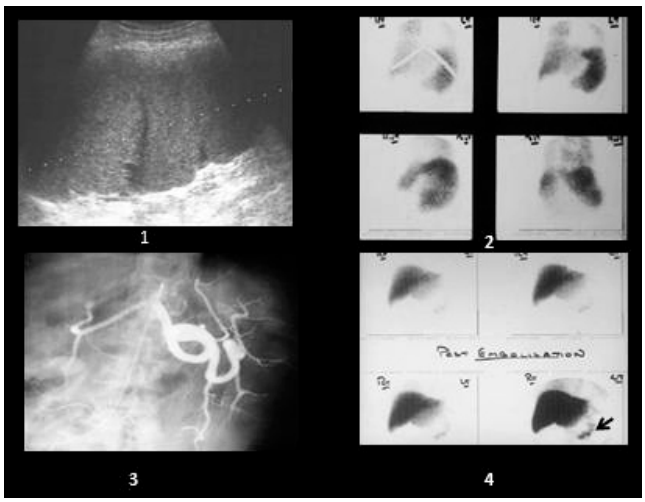

Figure 9 *Images from a 79-year old woman with a long history of rheumatoid arthritis and splenic amyloid and hypersplenism requiring blood transfusions every few weeks. As the patient was not fit for splenectomy splenic embolization was arranged. Image 1 is an ultrasound depicting splenomegaly. Image 2 is a colloid liver and spleen scan showing splenomegaly and colloid shift. Image 3 is pre-embolization angiogram. Image 4 is post embolization colloid scan showing a fraction of splenic tissue left. A colloid scan following splenic embolization represents an important imaging procedure as it shows the residual functioning splenic tissue and is more tissue specific than anatomical imaging*

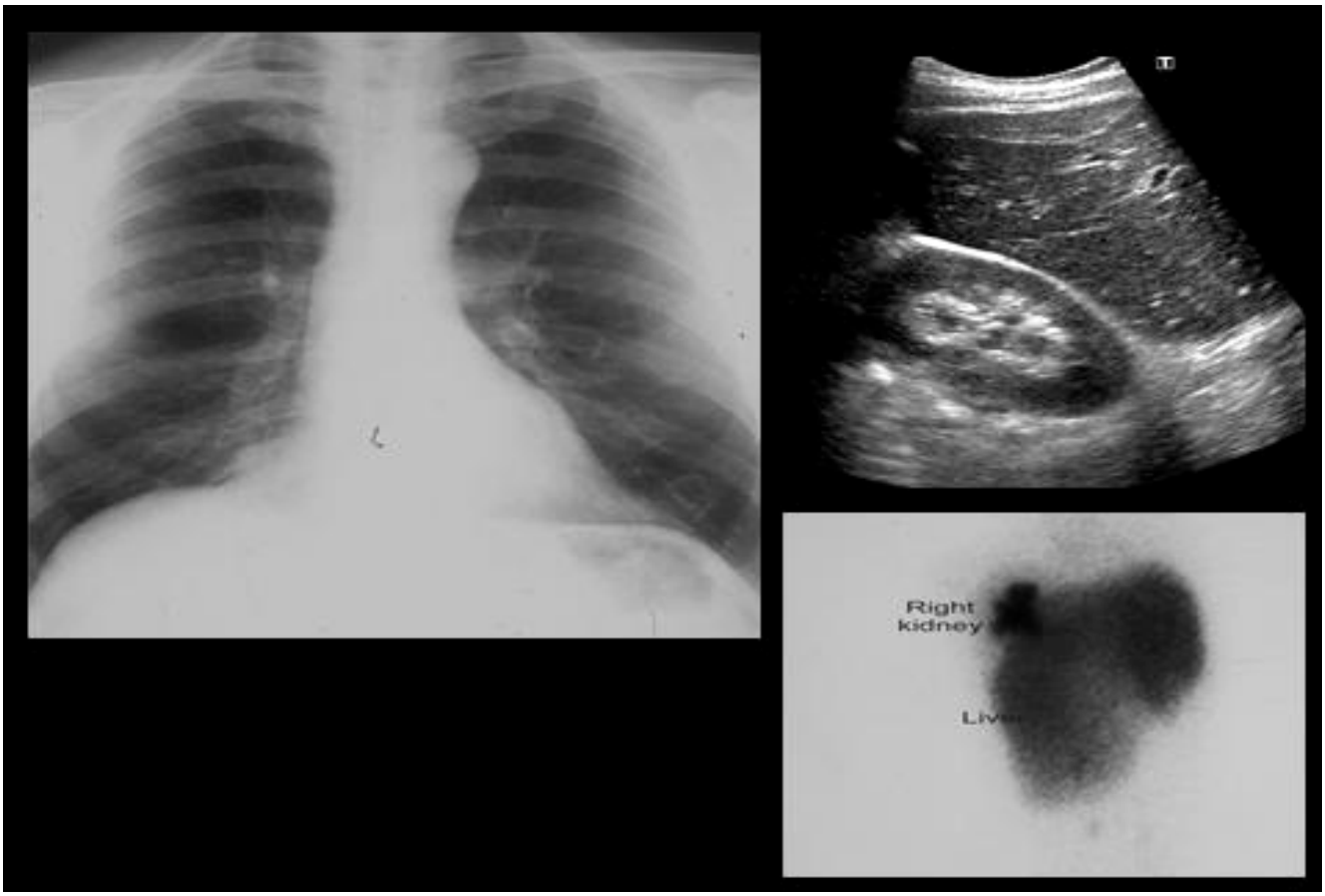

Figure 10 *Tissue diagnosis of renal herniation in a Bochdalek hernia by combined DTPA and Colloid scan*

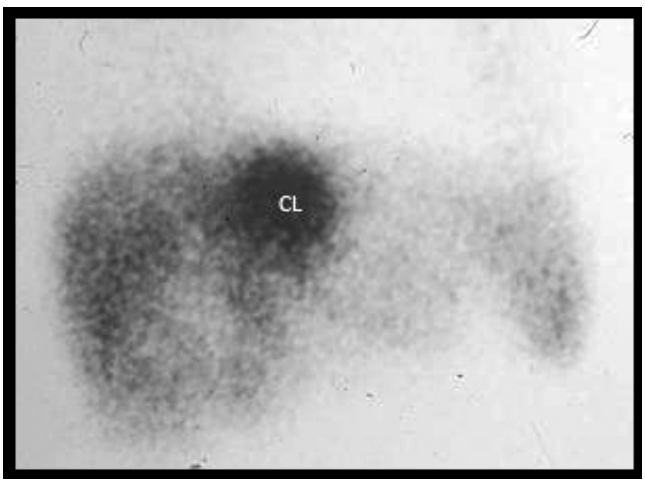

Figure 11 *An older sulphur colloid scan showing features of a Bud Chiari syndrome. Note relatively poor radionuclide uptake within the liver, with a hot enlarged caudate lobe (CL) with increased activity and mild splenomegaly*

A heat-damaged red blood cell scan can rule out an accessory spleen as a cause of upper abdominal mass. A case report describes a 34-year-old woman referred for evaluation of an abdominal mass seen at CT as a large mass in the region of the left hepatic lobe and adjacent to the spleen. A liver-spleen scan with sulphur colloid did not clearly show whether the mass originated in the liver or the spleen. A selective spleen scan using Tc-99m-labelled heat-damaged red blood cells showed intense uptake in the region of the spleen only so excluding an accessory spleen. The patient underwent surgical exploration and excision of the lesion, which proved to be focal nodular hyperplasia of the liver [11].

Laparoscopic excision of retained splenic tissue is advocated for recurrent haematologic disease after conventional splenectomy.

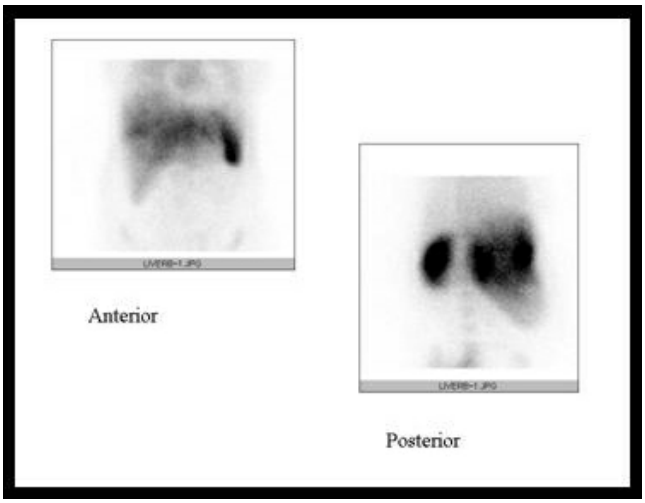

Figure 12 *Technetium-99m sulphur colloid scan of the liver shows peripheral areas diminished uptake due to liver atrophy and intense activity in the caudate lobe due to hypertrophy in a patient with Budd Chiari syndrome*

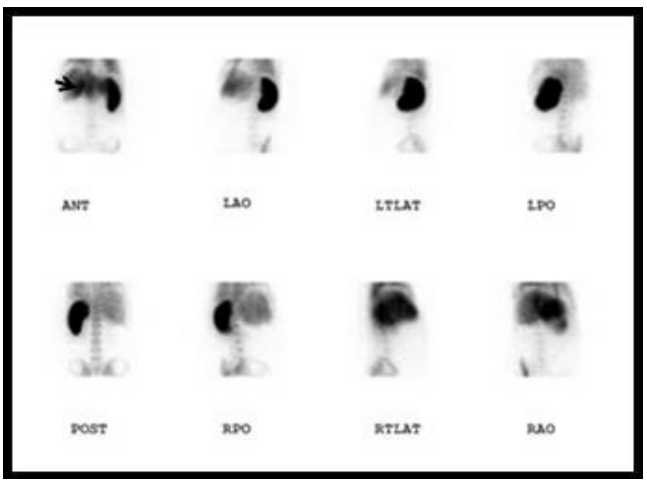

Figure 13 *Colloid scan shows increased uptake in the caudate lobe superimposed upon liver dysfunction (colloid shift) and splenomegaly in Budd Chiari syndrome*

However, intraoperative identification of residual splenic tissue remains difficult, especially when preoperative CT or MRI results are ambiguous or unremarkable. A successful laparoscopic excision of retained splenic tissue using technetium-99m sulfur colloid injection and intraoperative gamma probe localization has been reported in patients with recurrent idiopathic thrombocytopenic purpura [17-18].

Novel Applications of SCS

Non-alcoholic steatohepatitis (NASH) is associated with diffuse fatty infiltration and Kupffer cell dysfunction. Liver biopsy remains the diagnostic 'gold standard' in NASH. However, a liver biopsy is invasive and has other limitations. Colloid scintigraphy can register Kupffer cell activity and may be used to assess NASH. Altered liver right/left lobe ratio is found in the majority of NASH patients. Other common scintigraphic features of NASH include colloid shift to spleen and prolonged blood pool clearance time [1].

Interferon (IFN) is used as an effective treatment in some patients with chronic hepatitis (CAH). Presently there is no preliminary investigation to differentiate responders from non-responders. Caglar and associates evaluated the potential value of Tc-99m sulphur colloid liver/spleen and Tc-99m-disofenin hepatobiliary scintigraphy to predict treatment response to IFN in patients with CAH. Ten patients with chronic viral hepatitis B were recruited in the study had received 4.5 units of interferon alpha for 12 months. On SC scintigraphy, the liver/spleen percentage of non-responders was significantly lower than responders (median values: 0.69 vs. 1.16, p = 0.01), but, on hepatobiliary scintigraphy, no statistically significant parameters were found to predict response to interferon therapy [2].

Hepatobiliary Scintigraphy

See images Figures 15-32

Acute acalculous cholecystitis

Acute acalculous cholecystitis (AAC) is associated with a high mortality and remains an elusive diagnosis because of the complex clinical setting in which this entity develops. AAC is most often associated with the critically ill , making a definitive diagnosis difficult but

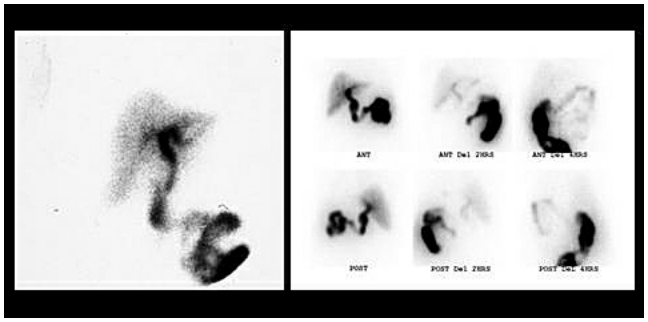

Figure 14 *HIDA in acute cholecystitis shown on two generations of gamma cameras. The patients presented with non-specific abdominal pain. Ultrasound showed no gallstones but gallbladder wall thickening. Both patients were shown to have acalculus acute cholecystitis at surgery. Note non-filling of the gallbladder on delayed scans*

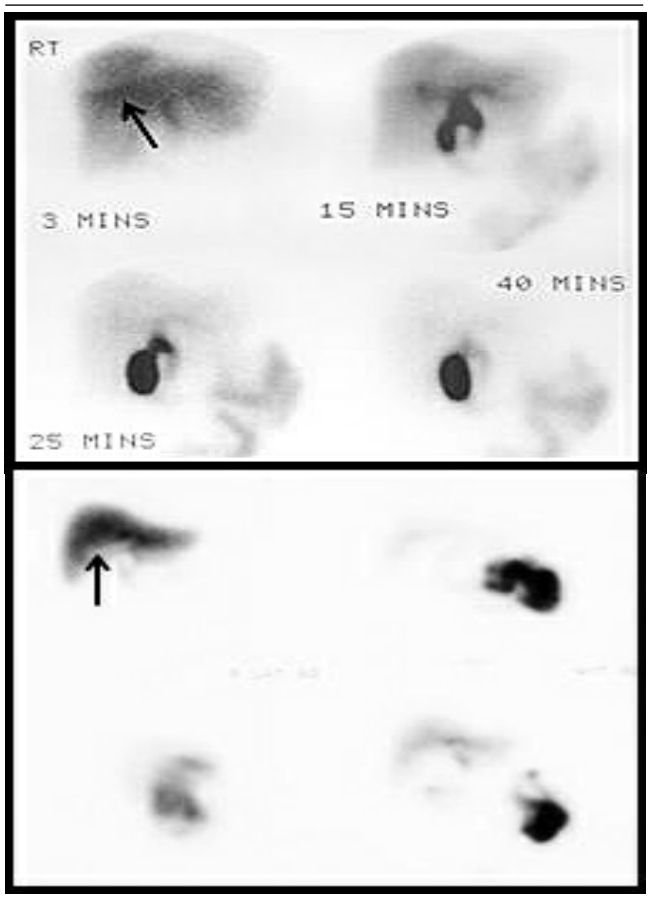

Figure 15 *Two generations of gamma cameras showing 'the rim sign' in acute cholecystitis*

imperative. Diagnosis of ACC is imaging based. Ultrasound (often sequential) and HIDA scans are the most reliable modalities for diagnosis. Cholecystectomy is the definitive treatment for AAC. However, at times image guided diagnostic/therapeutic drainage may be necessary and life saving, and may be the only treatment needed [32].

Sphincter of Oddi dysfunction

The diagnostic efficacy of quantitative hepato biliary scintigraphy (QHBS) was compared with that of endoscopic sphincter of Oddi (SO) manometry (ESOM) in patients with a suspected SO, dysfunction (SOD) of biliary type II or III. A significant correlation has been established between the trans-papillary bile flow measured by QHBS and the SO basal pressure determined by ESOM. QHBS can be used as a diagnostic method for the selection of SOD patients with an elevated SO basal pressure [41].

Bile Leaks

Hepatobiliary scintigraphy (HBS) is an important indication in post-traumatic biliary leaks. Mittal *et al.* retrospectively analysed 35 patients with abdominal trauma and found that HBS facilitates quick and accurate diagnosis of bile leaks.

Fleming and associates looked at 40 patients who underwent HBS after trauma. The results were classified as free intraperitoneal bile leak, contained bile leak, and no bile leak. Outcomes measured were length of hospital stay, number of procedures required, and number of subsequent imaging studies. Bile leaks were identified in 25% of patients. 8% had free intraperitoneal leaks, 18% contained bile leaks and 73% had no bile leak. Only one study was non-diagnostic due to reduced hepatic function. Free bile leaks had mean hospitalization of 53 days; contained bile leak group, 10 days; and no bile leak group, 14 days.

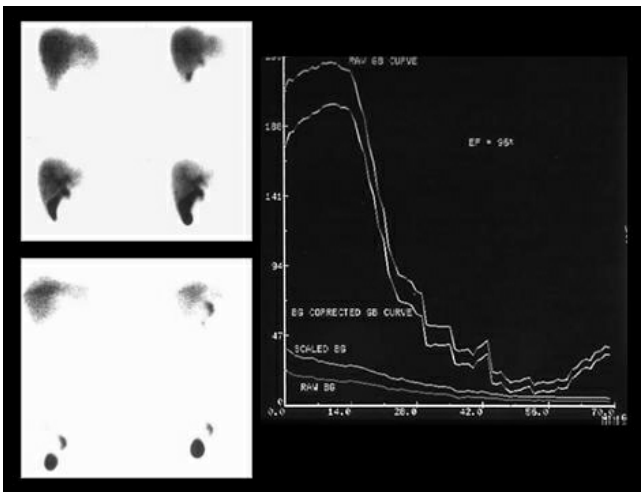

Figure 16 *Images with HIDA showing features of biliary dyskinesia*

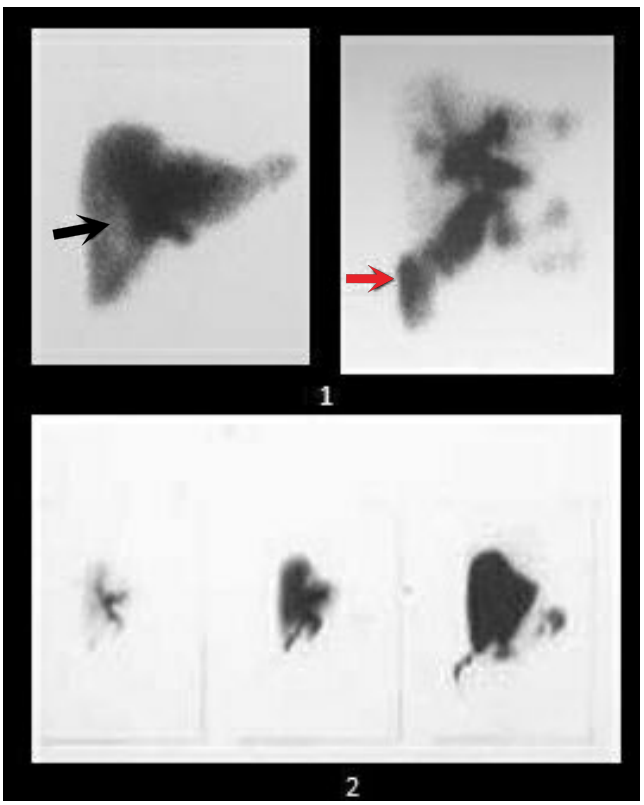

Figure 17 *HIDA scans on two different patients: Image 1 shows a traumatic liver tear seen as a photon deficient mass on the earlier scan (black arrow) followed by a delayed image showing bile leak (red arrow)*

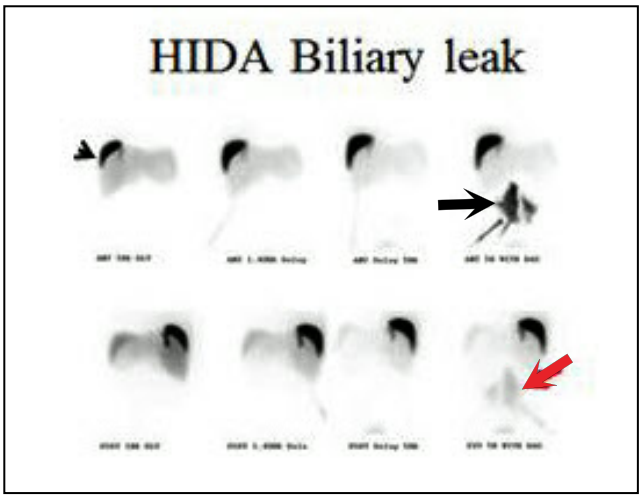

Figure 18 *A patient with bile duct injury and bile peritonitis. HIDA scan shows a bile collection into the subphrenic space (black arrow) and leak into the peritoneum on delayed images (red arrow)*

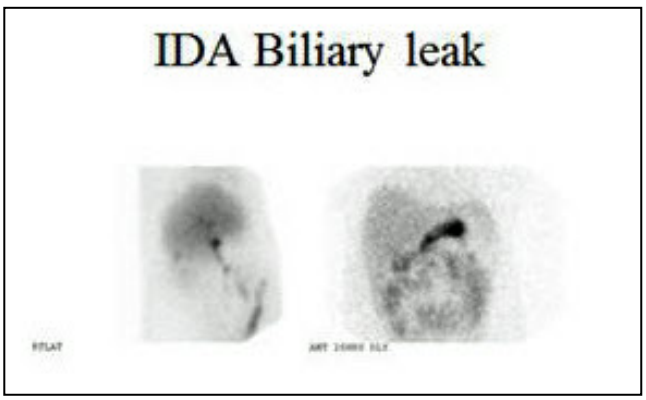

Figure 19 *IDA scan images show bile leak into the peritoneum following bile duct injury*

Bile duct injury and bile leaks are common and significant complications of cholecystectomy. The most common sites of bile leaks are the gallbladder fossa, the sub-hepatic space, in a bilioma, right paracolic gutter, or diffusely in the peritoneal cavity. Rarely bile leaks into the lesser sac may present a diagnostic challenge. Balakrishnan et all describe 6 patients where a definitive diagnosis was achieved by HBS. Any persistent focal radiotracer activity in the region of the lesser sac increasing with time

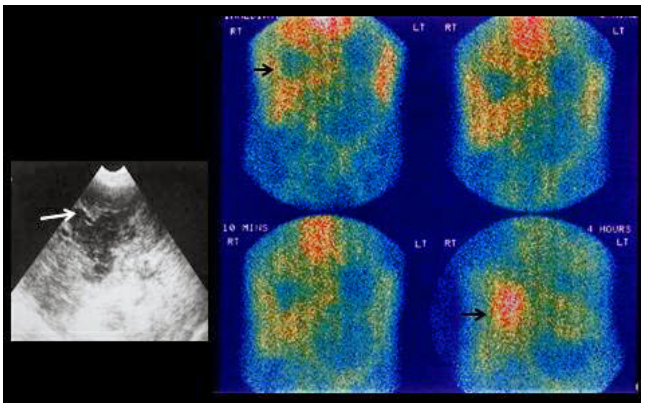

Figure 20 *HIDA scan shows a biloma following a liver biopsy. The early images show a photon deficient mass, which fills with radioactive bile on the 4 hour delayed image. Ultrasound scan shows a non-specific cystic lesion*

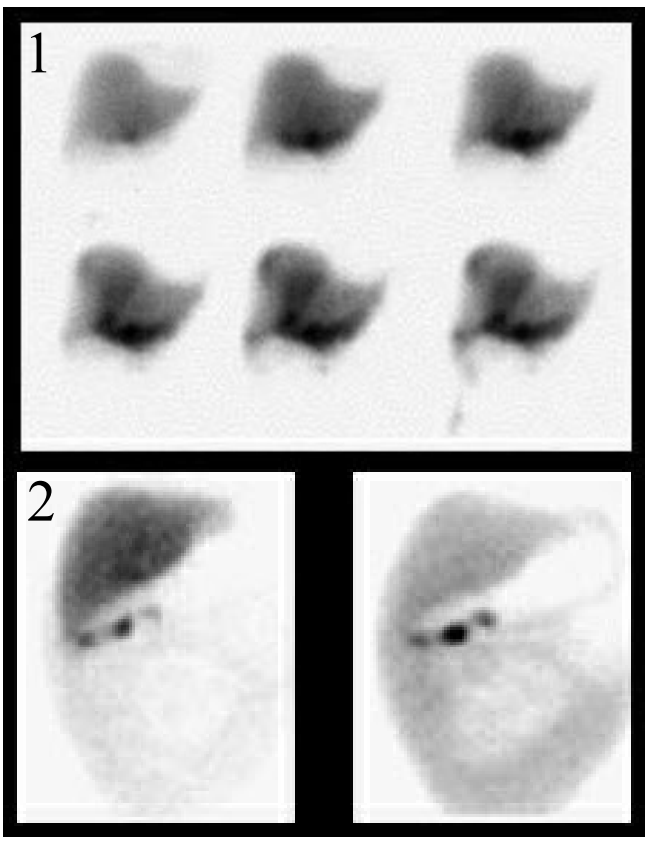

Figure 21 *HIDA scan showing a bile leak following a liver transplant on planar images (1) and SPECT images (2)*

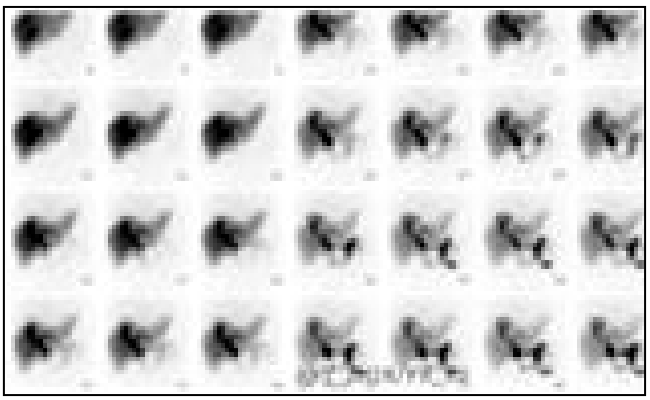

Figure 22 *Broncho-biliary fistula may occur spontaneously as a complication of liver hydatid cyst or following surgery for a liver hydatid cyst as in this patient*

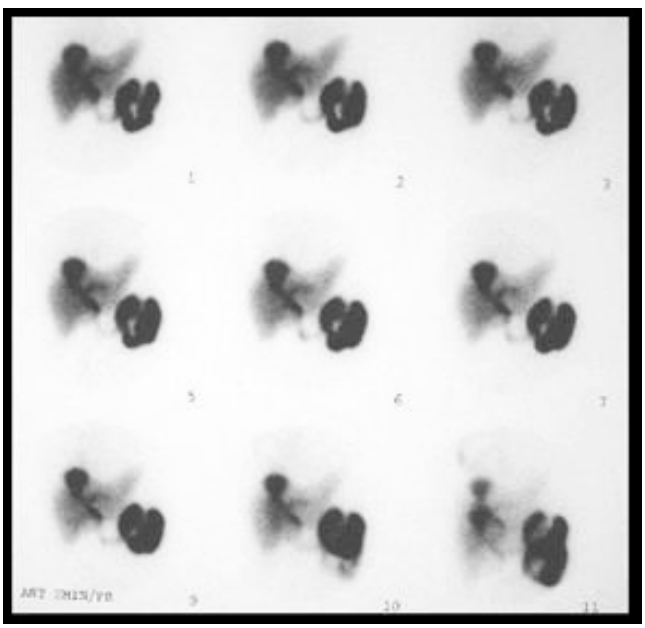

Figure 23 *Serial images show no biliary leak in the abdomen (image of the same patient as in Figure 22*

and not diffusing into the general peritoneal cavity is diagnostic of bile leak into the lesser sac [35].

Bile leaks and bile duct injury are serious postoperative complications of laparoscopic cholecystectomy. HBS is a valuable non-invasive method of investigating possible bile leaks or other biliary duct injuries following

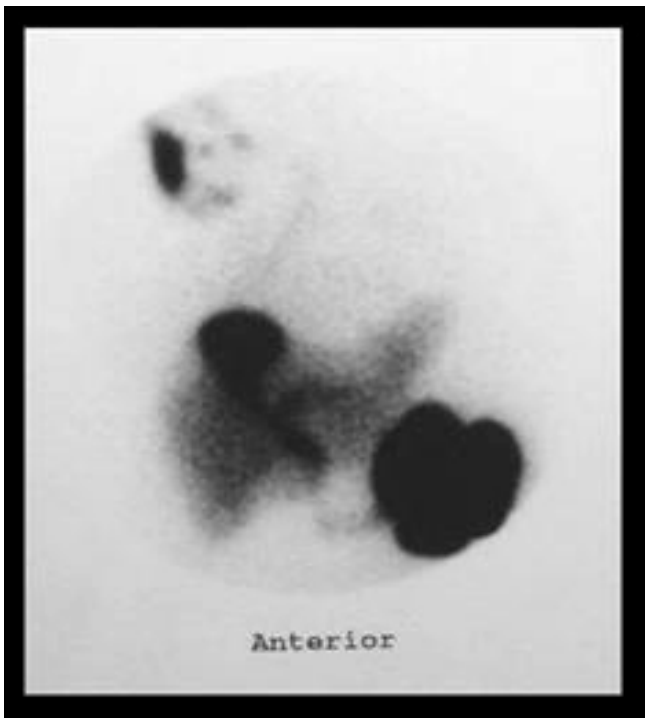

Figure 24 *Spot delayed image of the same patient as in Figures 22 & 23 shows tracer in the chest*

laparoscopic cholecystectomy. A negative study for significant bile leak is reassuring and would encourage conservative management. However, both false-negative and false- positive studies can occur [33-36].

Biliary complications are common after liver transplantation. HIDA scans are a non-invasive, reliable modality for early elimination of post transplantation biliary complications. However, clinical correlation is necessary to clarify imaging findings accurately. The sensitivity and specificity of HIDA scans to identify overall postoperative complications were 100% and 66.7%, respectively. False positive diagnosis for bile leak can occur in approximately 70% patients. Detection of obstruction is 75% sensitive by HIDA [37].

Hepatobiliary scintigraphy is able to assess grafts in the early postoperative period following liver transplants from living related donors. Gencoglu *et al.* examined 56 living related liver transplant recipients in the early postoperative period by hepatobiliary scintigraphy. Forty-four of the recipients were perfectly normal in the early postoperative period. Six recipients showed parenchymal dysfunction. In these patients, histopathologic endorsement by biopsies revealed four cases of hepatocellular damage/cholestasis, one acute rejection, and one cholangitis. Three patients demonstrated hypoactive areas in the liver graft, which when subjected to CT angiography (CTA) showed minor vascular problems. Three patents with normal parenchymal function scintigraphically, images were interpreted to indicate bile leak because accumulation of tracer was seen at an abnormal physiological site [38].

HBS is a commonly performed imaging technique on liver transplant patients to eliminate biliary obstruction or leaks. Biliary reconstruction in liver transplant patients is by either a choledochocholedochostomy or a Roux-en-Y hepaticojejunostomy. In patients with Roux-en-Y, hepaticojejunostomy radionuclide activity may be retained in the blind end of the Roux limb (the "blind end sign"). This activity often simulates a bile leak, which should be borne in mind when interpreting the results of HBS. Certain characteristic features, as well as delayed imaging, may aid in distinguishing the two such as variation in size and/or intensity with time [39].

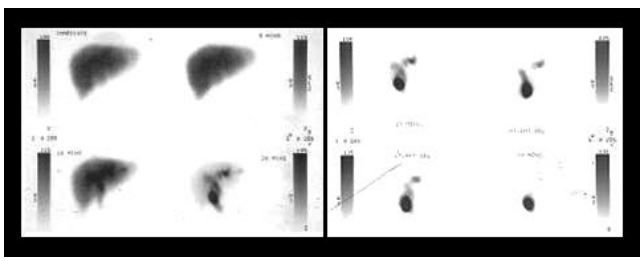

Figure 25 *Fibrocystic disease is a known cause of hepatobilary dysfunction. These HIDA images show delayed biliary excretion and bile duct strictures within the left lobe of the liver on HIDA scans in fibrocystic disease*

HIDA in hepatic fibrosis

A liver biopsy remains the gold standard in the staging of liver fibrosis in chronic hepatitis C virus (HCV) infection; several non-invasive techniques have been devised to assess the

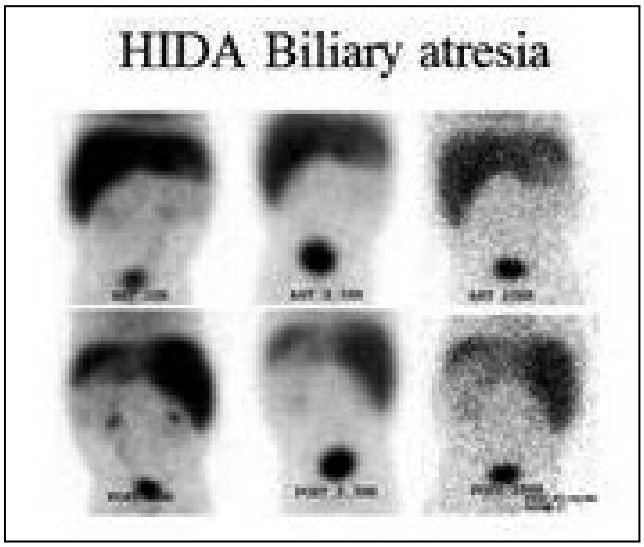

Figure 26 *HIDA in biliary atresia (anterior and posterior projection images). Ultrasonography is often the initial investigation in patients with suspected biliary atresia, followed by hepatobiliary scintigraphy. If the diagnosis remains elusive after these studies magnetic resonance cholangiopancreato graphy (MRCP) may be helpful. Laparoscopy and intraoperative ultrasound is being used with increasing frequency*

extent of hepatic fibrosis in HCV. A significant correlation exists between hepatobiliary function as assessed by technetium-99m-N-(-3-bromo-2, 4, 6-trimethylacetanilide) imino diacetic acid (Tc-mebrofenin) scintigraphy and the severity of liver fibrosis in patients with HCV [40].

Role of radionuclides in benign liver t*umours*

Cavernous haemangioma

Cavernous hemangioma is the most common primary liver tumour; its occurrence ranges from 0.4-20% (56). Cavernous hemangiomas arise from the endothelial cells that line the blood vessels and consist of multiple, large vascular channels lined by a single layer of endothelial cells and supported by collagenous walls. Cavernous hemangiomas are discovered

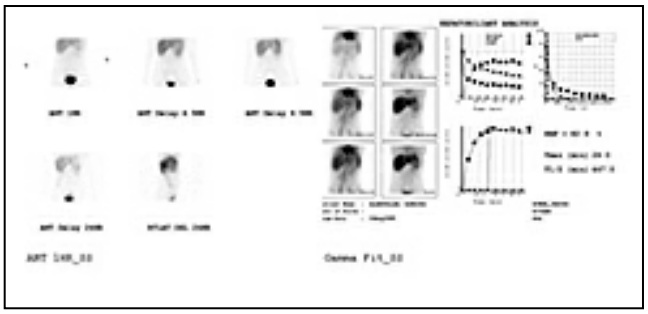

Figure 27 *No excretion through biliary system, even at 24 hr, is the most common finding. Extent of liver function damage may be assessed by quantifying the extraction efficiency*

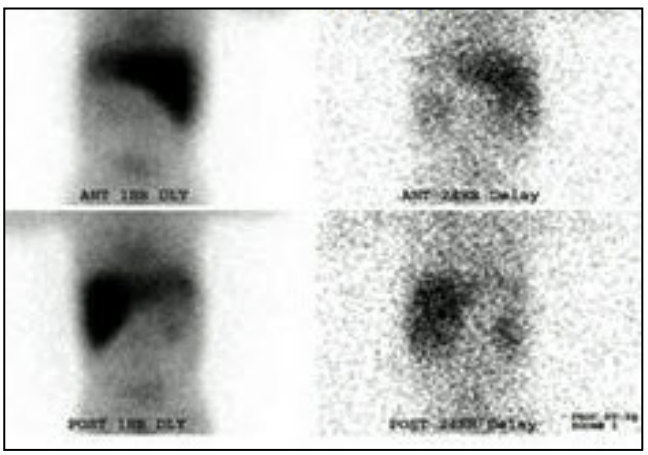

Figure 28 *HIDA images can spring up surprises; here are images from a 6-week-old baby boy showing not only features of biliary atresia but also situs inversus*

incidentally and are frequently asymptomatic. Hemangiomas are uncommon in cirrhotic livers; the fibrotic process in cirrhotic liver may prohibit their development (56). Most hemangiomas are incidentally detected on imaging. Ultra sonography is a cost-effective imaging modality for the diagnosis of a hemangioma. However, CT/or MRI may be required to specifically diagnose a hemangioma. However, the hypervascular nature may create equivocal findings on CT or MRI. SPECT imaging with ^{99m}Tc labelled red blood cell permits a specific diagnosis of haemangiomas.

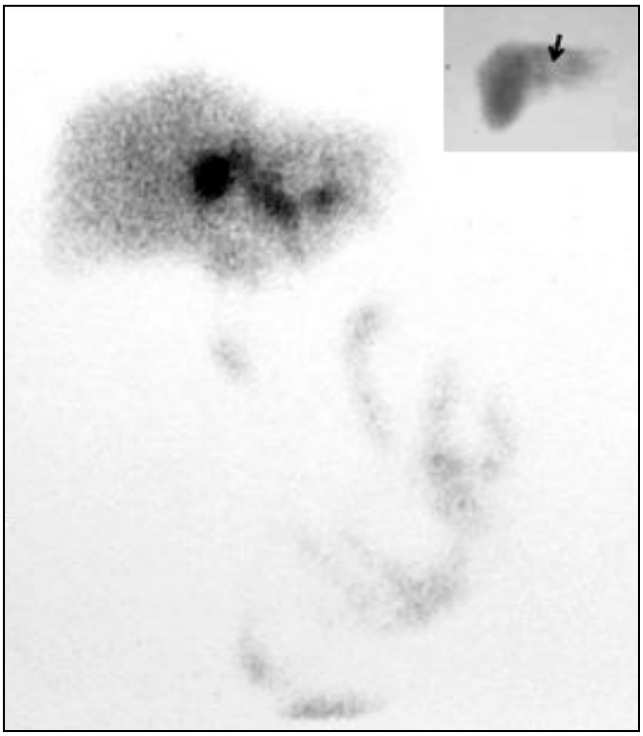

Figure 29 *HIDA scan on a patient with recurrent attacks of cholangitis and gram-negative septicaemia following a road traffic accident 6 years earlier. Image 1 (top right) shows photon-deficient areas in the left lobe of the liver on the hepatogram phase (arrow). Main image in the excretory phase show intense activity in a dilated left hepatic duct interspersed with strictures*

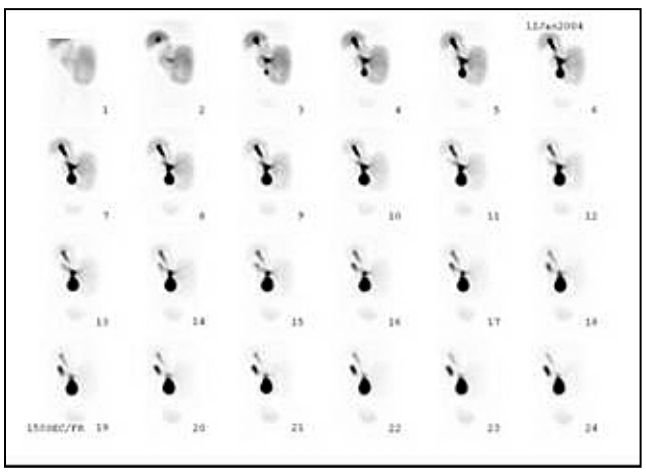

Figure 30 *Images of tissue specific diagnoses of duplication of the liver has been provided by a HIDA scan*

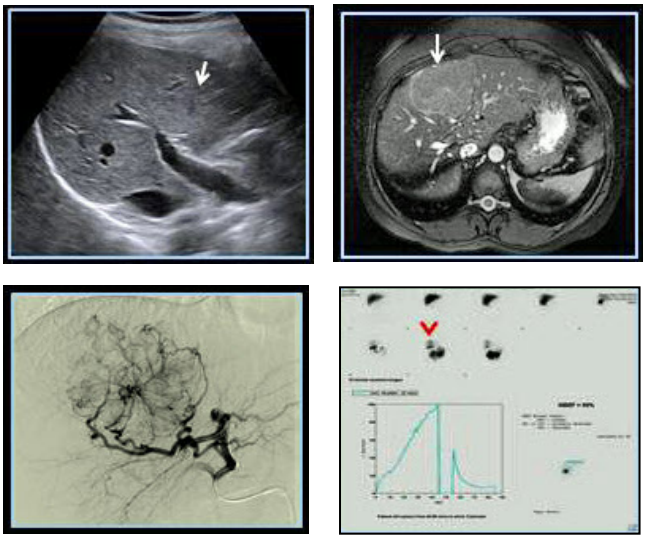

Figure 31 *This 16-year–old female presented with nonspecific right upper quadrant discomfort. The gallbladder was normal on ultrasonography, but a question of biliary dyskinesia was made and hence ejection fractions were calculated, which showed a normal study apart from focal activity within the liver (red arrow). US, contrast enhanced MRI and angiographyy showed characteristic appearances of FNH*

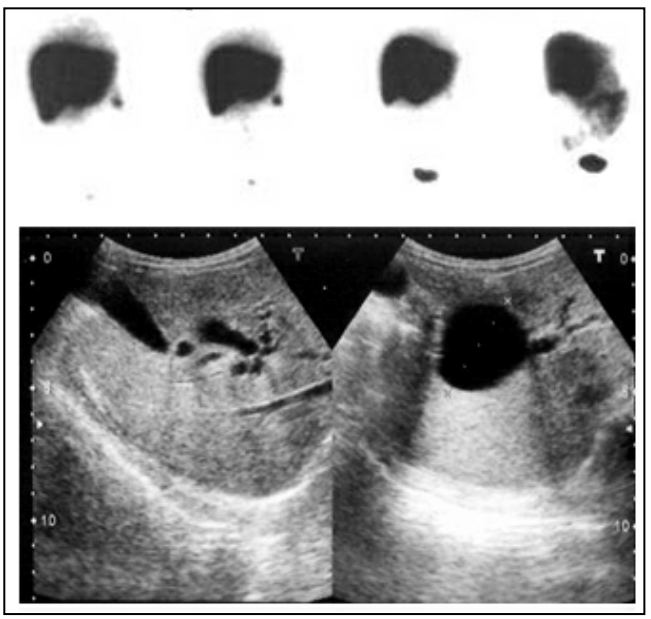

Figure 30x *Hepatobiliary scan top and ultrasound images showing choledochal cyst*

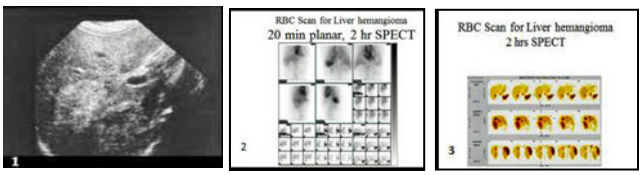

Figure 32 *These images are from a patient being staged for a primary malignancy. The ultrasound scan of the liver (1) showed a mixed echogenicity mass predominantly echogenic. The CT scan showed (not shown) a 4x3.5 cm mass that showed peripheral enhancement that was not characteristic of a haemangioma. Images 2 & 3 depict planar and SPECT images showing a complete 'fill-in' of the mass with labelled red blood cells, characteristic of a haemangioma. The use of nuclear medicine show how the patient is prevented from more expensive and invasive techniques*

Although FNH usually has no clinical significance, recognition of the imaging characteristics of FNH is essential to avoid unnecessary surgery, biopsy, and follow-up imaging. The diagnosis of FNH is made on the demonstration of a central scar; however, a typical central scar is not demonstrated in every patient. In as many as 20% of patients, a scar may not be visible. Moreover, a central scar may be found in some patients with fibro lamellar hepatocellular carcinoma, hepatic adenoma, or intrahepatic cholangi carcinoma. This limitation applies to all cross-sectional imaging techniques. The detection of lesions by use of radionuclide scans with technetium-99m sulphur colloid depends on the concentration of Kupffer cells in the FNH. If the concentration of Kupffer cells is low, FNH may appear as a photon-deficient mass that is indistinguishable from other liver mass lesions (Figure 32).

The diagnosis of FNH is achieved by the use of several complementary imaging techniques. Patients in whom the diagnosis is not clearly determined with imaging findings, open biopsy or surgical resection may be needed; findings on needle biopsy may substantially overlap with those of well-differentiated hepatocellular carcinoma [59-62]. The best imaging modalities for characterizing FNH are those modalities which can delineate the lesion's central scar or that can show Kupffer cell activity. The best modalities for identifying the central scar are CT and MRI; Kupffer cell activity is best demonstrated by radionuclide scans. In the future however, MRI super paramagnetic contrast agents may challenge radionuclide scanning.

Detection of Kupffer cells in FNH has historically been achieved using technetium-99m sulphur colloid scanning (see the image below). In 60-70% of FNH patients, these scans show normal or increased uptake of99m Tc sulphur colloid. In 30-40% of patients, Kupffer cells are not sufficiently concentrated in the FNH lesion; the lesion may even be photon deficient (63). The uptake of ^{99m}Tc-hepato iminodiacetic acid (HIDA) is normal or increased in 40-70% of patients, but the lesion may be photon deficient in as many as 60% of patients. With ^{99m}Tc-tagged RBCs, uptake is increased during the early phase; subsequently, the uptake is decreased (63). ^{99m}Tc sulfur colloid uptake in patients with FNH depends on the concentration of Kupffer cells in the FNH lesion. Unfortunately, other hepatocellular neoplasms, such as a hepatocellular adenoma and hepatocellular carcinoma, may also have Kupffer cells and demonstrate ^{99m}Tc sulphur colloid uptake. Hepatic adenoma, haemangioma, hepato blastoma, liver herniation, and hepatocellular carcinoma may be similar in appearance on ^{99m}Tc sulphur colloid scans.

Benign solid liver tumours

The modalities currently available in imaging for the detection and characterisation of liver masses include ultrasound/colour Doppler sonography, CT, MRI, radionuclide scinti graphy (Technetium RBC, sulphur-colloid, IDA scan), angiography, and image-guided percutaneous needle biopsy. MRI is probably better at characterizing lesions than CT, but CT is the preferred modality of choice at many institutions due to the speed of acquisition and good contrast resolution inherent in the

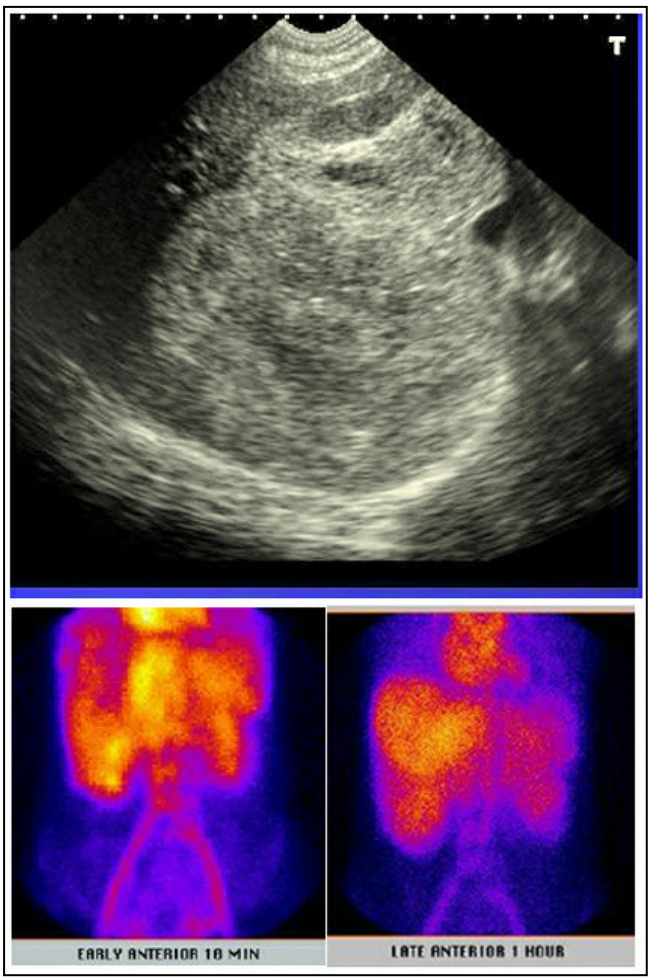

Figure 32 *These images are from a patient being staged for a primary malignancy. The ultrasound scan of the liver (1) showed a mixed echogenicity mass predominantly echogenic. The CT scan showed (not shown) a mass that showed peripheral enhancement that was not characteristic of a haemangioma. The blood pool images (bottom) show complete 'fill-in' of the mass with labelled red blood cells, characteristic of a haemangioma. The use of nuclear medicine show how the patient is prevented from more expensive and invasive techniques*

Although FNH usually has no clinical significance, recognition of the imaging characteristics of FNH is essential to avoid unnecessary surgery, biopsy, and follow-up imaging. The diagnosis of FNH is made on the demonstration of a central scar; however, a typical central scar is not demonstrated in every patient. In as many as 20% of patients, a scar may not be visible. Moreover, a central scar may be found in some patients with fibro lamellar hepatocellular carcinoma, hepatic adenoma, or intrahepatic cholangi carcinoma. This limitation applies to all cross-sectional imaging techniques. The detection of lesions by use of radionuclide scans with technetium-99m sulphur colloid depends on the concentration of Kupffer cells in the FNH. If the concentration of Kupffer cells is low, FNH may appear as a photon-deficient mass that is indistinguishable from other liver mass lesions (Figure 32).

The diagnosis of FNH is achieved by the use of several complementary imaging techniques. Patients in whom the diagnosis is not clearly determined with imaging findings, open biopsy or surgical resection may be needed; findings on needle biopsy may substantially overlap with those of well-differentiated hepatocellular carcinoma [59-62]. The best imaging modalities for characterizing FNH are those modalities which can delineate the lesion's central scar or that can show Kupffer cell activity. The best modalities for identifying the central scar are CT and MRI; Kupffer cell activity is best demonstrated by radionuclide scans. In the future however, MRI super paramagnetic contrast agents may challenge radionuclide scanning.

Detection of Kupffer cells in FNH has historically been achieved using technetium-99m sulphur colloid scanning (see the image below). In 60-70% of FNH patients, these scans show normal or increased uptake of^{99m}Tc sulphur colloid. In 30-40% of patients, Kupffer cells are not sufficiently concentrated in the FNH lesion; the lesion may even be photon deficient (63). The uptake of ^{99m}Tc-hepato iminodiacetic acid (HIDA) is normal or increased in 40-70% of patients, but the lesion may be photon deficient in as many as 60% of patients. With ^{99m}Tc-tagged RBCs, uptake is increased during the early phase; subsequently, the uptake is decreased (63). ^{99m}Tc sulphur colloid uptake in patients with FNH depends on the concentration of Kupffer cells in the FNH lesion. Unfortunately, other

technique. Nevertheless, several imaging techniques are used for specific radiologic findings to arrive at the diagnosis. In patients with atypical features, a definitive diagnosis is usually obtained by a needle biopsy. Recent developments in the application of specific ultrasound and MR contrast agents may find a role as problem-solving examinations after inconclusive ultrasound and helical CT [20].

Hepatic Adenoma

CT and MRI appearances of hepatic adenomas are highly variable and may be indist inguishable from those of other hepatic tumours. Kume *et al.* described two patients with hepatic adenomas with highly atypical CT and MRI manifestations demonstrating a "nodule-in-nodule" appearance. Ga-67 scanning in both patients showed decreased uptake in the adenomas compared to normal liver, negative colloid (^{99m}Tc-phytate) uptake, and early uptake and subsequent retention of ^{99m}Tc-PMT. These scintigraphic characteristics correctly predicted the diagnosis of the hepatic adenomas. Scintigraphic studies in combi nation may play an important role in aiding the diagnosis of this rare benign tumour, despite variable CT and MRI appearances [21].

Several available modalities may be needed to arrive at a confident diagnosis of the actual benign liver mass; the various features of these masses on presentation, NM, US and CT are given in table 1.

Focal fatty infiltration

Lisbona *et al.* studied 12 patients with sono graphic appearance of multiple focal nodules due to fatty infiltration of the liver. All twelve patients with such focally abnormal ultrasound images were referred for liver scintigraphy with ^{133}Xe and ^{99m}Tc colloidal SPECT studies. In 9 of the 12 patients, the innocent nature of the sonographic abnormalities, were related to a benign process of focal fat deposition. Furthermore, ^{99m}Tc-RBC scans showed genuine space-occupying lesions within the liver. Scintigraphy has an important role in the defining of focal hepatic ultrasound abnormalities particularly in unsuspected hepatic steatosis [22]. See Figure 9.

Managing malignant disease

Liver metastases

Hepatic arterial perfusion scintigraphy

The importance of detection of accurate liver metastases from colorectal carcinoma cannot be overemphasized. Approximately a third of patients undergoing hepatic resection for colorectal metastases are known to have occult metastases at the time of surgery that are not detected with cross-sectional imaging or sulfur colloid scanning (64-65). These patients may benefit from CT arterioportography (CTAP). CTAP works on principles similar to those of hepatic artery perfusion scintigraphy (HAPS). The study involves the infusion of technetium-99m (99m Tc) macroaggregated albumin into a hepatic artery catheter. Metastases appear as areas of increased focal radionuclide uptake. SPECT following HAPS may show metastatic lesions as small as 0.5-1 cm. In a prospective study, Vogel and associates compared preoperative HAPS with CTAP and found sensitivities of 92% and 86% and positive predictive values of 73% and 60%, respectively. HAPS showed more metastases; some of the lesions were not apparent at surgery, and blind biopsy was needed for confirmation. HAPS have a false-positive rate of 25%. How many of these lesions are truly false positive is not known because patients with lesions deemed inoperable seldom undergo follow-up imaging. Describing the experience at one center, Drane (66) showed that almost 50% of the lesions classified as false positive were later proved liver metastases. Vogel et al investigated 48 patients with colorectal cancer that had laparotomy following a normal CT. The pre-operative investigation included a standard CT, CT arterial portography and HAPS using radiolabeled macroaggregated albumin. Early studies showed an increased sensitivity for detecting small lesions using

Table 1 *Differential diagnosis of cavernous haemangiomas, focal nodular hyperplasias and hepatic adenomas*

	Cavernous Haemangioma	**Focal nodular hyperplasia**	**Hepatic adenoma**
Clinical presentation	Can be solitary or multiple. Small tumours (<3cm) Always incidental, large tumours might present with pain. Sometimes thrombocyto penia due to sequestration	Usually solitary Incidental finding Most lesions <5 cm	Usually solitary and large (>8 cm). Commonly presents with pain and mass. Very large lesions possible.
Association	Women outnumber men by 5:1. Can enlarge in pregnancy or with oestrogen administration	Oral contraceptives and female gender have a weak association	Oral contraceptives have a strong association. Tumour might regress on stopping oral contraceptive. Glycogen storage disease.
Histopathology	Large vascular channels lined by single layer of endothelium, supported by a little fibrous tissue, might have thrombotic areas	Normal hepatocytes, Kuppfer cells, bile ducts, and portal triads, central fibrous scar often radiating	Normal hepatocytes with absent bile ducts. Most do not contain Kuppfer cells. Fat and calcification might be present.
Ultrasound	Small lesions are echogenic and sharply defined. Large lesions can be lobulated and have a relatively echogenic rim and irregular hypoechoic interior. Can appear completely hypoechoic in a fatty liver	Well defined almost isoechoic regular lesions, sometimes picked up only by mass effect rather than visualization of the mass itself. Lesions usually have a homogenous pattern.	Variable echogenicity from hypo to hyperechogenic. Hyperechogenic areas (due to calcification and fat) can suggest the right diagnosis. Might have a pseudocapsule. Can have complex fluid consistency central areas (intratumoural bleeding) and there can be free peritoneal fluid.
Colour Doppler	No flow identified on Doppler	Vascular with central as well as peripheral vessels, spoke-wheel pattern is very suggestive. Large feeding artery is characteristic but not invariable	Vascular but more venous vessels than arterial as compared to FNH.
Nuclear medicine	Cold on colloid liver scan. Cold on early blood pool scan. Hot on late blood pool study.	Variable on colloid scan, but most will be warm or hot. This is characteristic. Some are cold and need further investigation. This depends upon Kupffer cell density	Cold on colloid scan, hot on hepatobiliary HIDA scan
Computed tomography	Contrast fills in from the periphery (centripetal filling in)	Somewhat hypodense. Hypervascuar, with capillary stain, central feeding vessel is characteristic	Haemorrhage if present can be seen on noncontrast images. Can have portal venous washout

the invasive CTAP. Similarly, the HAPS study has detected malignant lesions not observed by standard CT. However, False-positive studies were reported with both HAPS and CTAP, which may limit the ability of these tests to accurately predict unresectability before operation and may deny patients the chance for surgical resection. False-positive lesions after CTAP included haemangiomas, cysts, granulomas, and flow artifacts. The HAPS study however, detects small lesions not seen by CT or CTAP.

The hepatic perfusion index has been used to evaluate occult liver metastases. The technique involves dynamic hepatic scintigraphy, which provides an estimate of the ratio of the total arterial blood flow to the total liver blood flow; this ratio is known as the hepatic perfusion index. Some believe that an increased hepatic perfusion index is associated with occult liver metastases, whereas others maintain that a low index is more important. A low index suggests that the patient is at a low risk for metachronous tumours, and therefore, they may be spared from adjuvant chemotherapy.

Other applications of HAPS include assessment of liver perfusion and its alteration in various hepatic diseases. It measures the arterial and portal venous fractions of total liver blood flow. The hepatic arterial flow is calculated mathematically by the hepatic perfusion index (HPI), normally between 25 % and 40 %. The decrease of portal blood flow in liver cirrhosis is compensated by an increased arterial supply, with higher HPI value. In patients with chronic liver disease such as cirrhosis, an HPI over 50% suggests arterialization of hepatic perfusion. Malignant liver tumours increase the liver arterial flow and decrease the portal flow. The HPI varies between 65-90%. Benign liver tumours do not change portal/arterial hepatic blood ratio. HAPS-SPECT enhances its diagnostic value in primary liver tumours, although HAPS in HCC has limitations due to underlying cirrhosis. Hepatic metastases increase the arterial perfusion and HPI value early, before their size allows morphologic imaging diagnosis. HAPS is therefore an early method to diagnose liver metastases being especially used in colorectal cancer. HAPS has also been used for follow up of liver toxicity of drugs, evaluation of portal vein permea bility, post-surgery follow up of the liver tumour patients [67].

FDG PET

Current imaging strategies fail to detect occult liver and extra-hepatic metastases, which explains the high rates of recurrence for colorectal cancer after liver resection. Although FDG-PET cannot match the anatomic resolution of cross-sectional imaging, it is particularly useful in the detection and characterization of extrahepatic disease that may not be identified on cross-sectional imaging [68].

Rohren *et al.* [69] have shown that in patients being evaluated for potential curative resection of hepatic metastases from colorectal cancer, FDG PET is accurate for identifying metastatic disease to the liver. The sensitivity and specificity of FDG PET are 95% and 100%, respectively. However, the detection of individual metastases depends on their size, and anatomic imaging methods such as intra-operative ultrasound (IOUS) more accurately depict their distribution and size. FDG PET is also more accurate than CT and carcinoembryonic antigen (CEA) studies for detection of recurrent colorectal cancer. The detection rate for liver metastases is generally better for CT than for FDG PET (80% vs 65%). This rate is related to tumour size; therefore, the false-negative rate is significant. Several sources of benign and physiologic increases in activity may yield false-positive results.

FDG PET and FDG PET/CT are effective in the identification of additional hepatic and extra-hepatic metastases, frequently upstaging the tumour and modifying treatment. PET-CT is also useful in local ablative and systemic therapy assessment and surveillance for liver metastases [70].

In a systematic review, Patel *et al.* concluded that PET/CT has a higher accuracy for detection

of extra-hepatic and hepatic colorectal metastatic disease than CT alone. However, the results are based on a small number of studies and should be interpreted with caution [71].

A meta-analysis undertaken by Maas *et al.* concluded that both whole-body PET and PET-CT were very accurate for the detection of local recurrence and distant metastatic disease in patients with colorectal cancer with a high suspicion of recurrent disease. CT was found to have the lowest diagnostic performance. The study analysis revealed that PET-CT might be the modality of choice when evaluating patients with a high suspicion of recurrent disease, because of its best performance in patient-based analyses and confident prediction of disease status [72].

Another meta-analysis looked at the diagnostic performance values of CT, MRI, FDG-PET, and FDG PET-CT in the detection of colorectal liver metastases in patients who had not previously undergone therapy. MRI was considered the preferred first-line modality for evaluating colorectal liver metastases in patients who had not previously undergone therapy. FDG-PET can therefore be used as the second-line modality [73].

A randomised controlled study [74] concluded that the number of futile laparotomies were reduced from 45% to 28%, by the addition of FDG-PET to the work-up for surgical resection of colorectal liver metastases, and thus prevented unnecessary surgery in one of six patients. The addition of FDG-PET imaging also significantly improves conventional staging by CT. Up to now, definitive evidence that the addition of ^{18}F-FDG PET to conventional staging leads to superior clinical results and improved clinical management in these patients has been lacking. See Figures 53-54.

^{18}F-DOPA PET

^{18}F-Dopa PET has proved useful in imaging primary and metastatic GI carcinoid tumours and their lymph node and organ metastases. In general, FDG-PET is useful in cases of poorly differentiated carcinoids and other neuroendocrine tumours, but it should not be used as a first-line imaging agent. FDG-PET is primarily useful when somatostatin receptor scintigraphy results are negative. ^{18}F-Dopa PET is a promising procedure and a useful supplement to morphologic imaging methods. FDG-PET imaging is useful in poorly differentiated carcinoids when somatostatin receptor scintigraphy results are negative.

^{18}F-DOPA-PET is a promising new diagnostic tool in the imaging of neuroendocrine tumours (NET). The application of ^{18}F-DOPA PET-CT in carcinoid tumours has unsurpassed sensitivity. In medullary thyroid cancer, pheo chromocytoma, and hyperinsulinism, results are also excellent and contribute significantly to clinical management. In other NET, the initial experience with ^{18}F-DOPA PET indicates that it seems to be less valuable, but further study is required [75].

In a prospective, single-centre, diagnostic accuracy study, ^{18}F-DOPA PET with carbidopa pretreatment was compared with somato statin-receptor scintigraphy (SRS), CT, and combined SRS and CT in 53 patients with a metastatic carcinoid tumour. The study revealed sensitivities of 100% for ^{18}F-DOPA PET, 92% for SRS, 87% for CT, and 96% for combined SRS and CT. ^{18}F-DOPA PET also detected more lesions, than combined SRS and CT. ^{18}F-DOPA-PET has the potential to replace conventional and SRS imaging and, help improve prediction of prognosis, and be used to assess patients' response to treatment for carcinoid tumours [76].

Recent advances in morphology-based imaging modalities have increased the sensitivity and specificity of detection of liver or pancreatic lesions. FDG-PET has proven sensitivity and specificity in the diagnosis of hepatic metastases and extra-hepatic tumour deposits from hepatocellular or pancreatic cancer. ^{18}F-FDG PET can increase the accuracy of staging of HCC and primary pancreatic

tumours and can be used for response monitoring. Ga-68 DOTATOC and F-18 DOPA allow detection of NET and their metastases. PET-CT and SPECT-CT allow integration of metabolic and morphologic and information, increasing diagnostic sensitivity and specificity and accurate anatomical localization [23].
Iodine-123-(S)-2-hydroxy-3-iodo-6-methoxy-N-[(1-ethyl-2-pyrrolidinyl) methyl] benzamide ([123I]-(S)-IBZM) uptake was evaluated in eleven patients with proven metastatic melanoma . The [123I]-(S)-IBZM scans allowed the detection of all six cutaneous lesions, five of six superficial pathologic lymph nodes, four of five pulmonary and one of two hepatic metastases [24].

Medullary thyroid carcinoma metastases

A variety of radionuclides may be used to detect medullary thyroid carcinoma and its metastases. These metastases may be imaged with ^{131}I-MIBG, ^{111}In-Octreotide, ^{99m}Tc-dimercaptosuccinic acid (V) (DMSA[V]), ^{201} Tl, ^{99m}Tc-Sestamibi, and FDG. Because sufficient experience has not been gained with any one agent and no comparative trial is possible, the choice of the agent to be used is determined on the basis of local expertise, availability, and cost. DMSA(V) and ^{201}Tl, or a combination of the 2 agents, is the least expensive agent and used in some centres [77].

Hepatocellular Carcinoma

Molecular imaging of HCC

Scintigraphy remains at the forefront of molecular imaging because of the relatively high sensitivity to detect nanomolar or picomolar quantities of the radio labelled imaging probe. Imaging has a fundamental role in the diagnosis of hepatocellular carcinoma. Nuclear imaging was one of the earlier modalities used in characterizing liver masses especially in HCC. The radionuclides used included ^{99m}Tc sulphur colloid, gallium-67, and ^{99m}Tc iminodiacetate acid analogues. Other radionuclides that can be used to assess functional liver volume include ^{99m}Tc diethylenetriamine pentaacetic acid-galactosyl-human serum albumin. 99mTc-labelled tetrofosmin and methox isobutylisonitrile, has been utilized to detect drug resistance. FDG-PET and carbon-11 labelled acetate appears to show improved sensitivity and specificity for HCC. Oxygen-15 PET is useful in the measurement of hepatic and tumour blood flow. The absence of specific molecular targets, problems with drug delivery, and poor contrast-to-noise are factors that have contributed to poor molecular imaging in the identification and characterization and treatment monitoring of HCC [26].

Microvascular invasion in HCC is a poor prognostic indicator of cancer recurrence after surgical treatment. Positron emission tomography (PET) with ^{18}F-flourodeoxy glucose (^{18}F-FDG) as a tracer has been employed to predict the prognosis before surgery for various kinds of tumours, but it has not been found to be sensitive enough for HCC. Thus, ^{11}C-acetate has been adopted as an additional tracer. A tumour size greater than 5 cm was significantly associated with positive ^{18}F-FDG PET results; ^{11}C]acetate was not associated with poor prognostic indicators. Preoperative ^{18}F-FDG PET may predict micro vascular invasion. The addition of ^{11} C-acetate improves the overall sensitivity of PET, but it has no incremental value in predicting microvascular invasion [55]. See Figure 51.

Tl-201 positive, Ga-67 negative hepatoblastoma

Thallium-201 uptake has been described in 12-year-old boy with a hepatoblastoma in whom Ga-67 scintigraphy and serum alpha-fetoprotein were negative. The use of Tl-201 scintigraphy should, therefore, be considered in children with indeterminate liver masses [25].

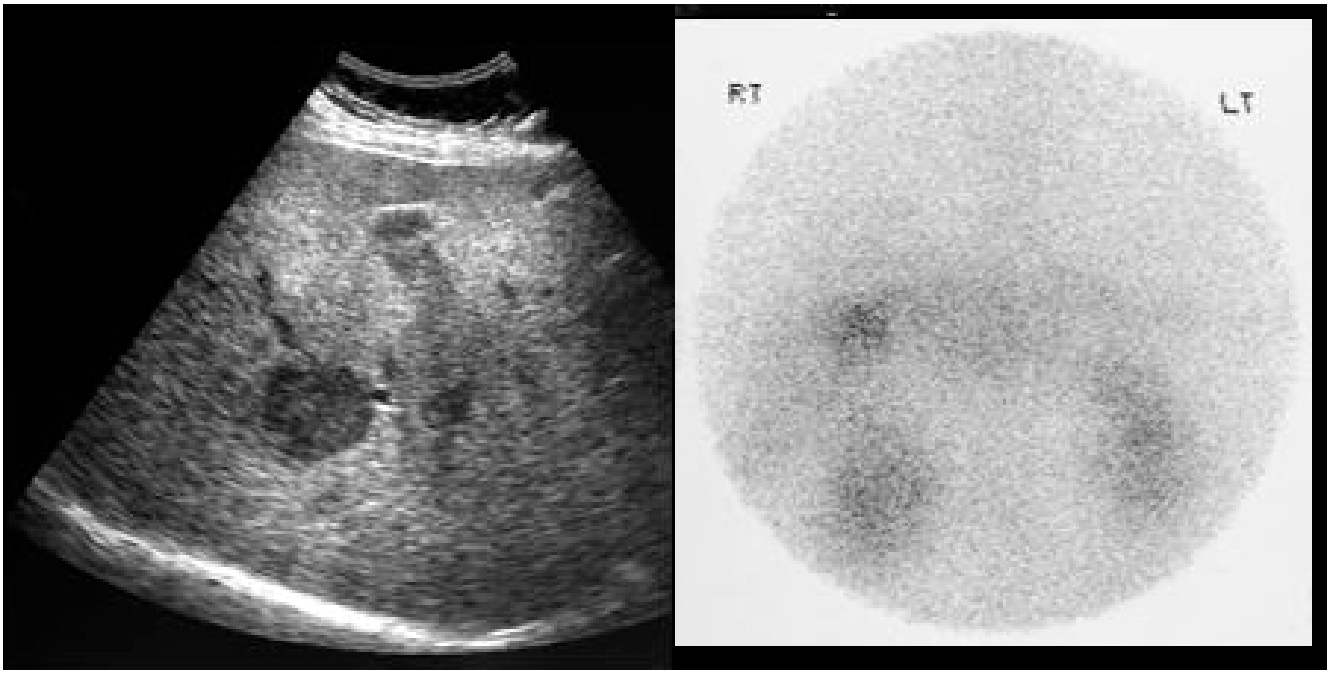

Figure 33 *Presently Octreotide scanning has gained a central role, in the diagnoses of carcinoid whereas anatomical studies serve for the completion of the oncologic work-up. Ultrasound image of a patient with raised ALT and alkaline phosphatase shows a hypoechoic mass within a fatty liver [1]. Most mass lesions within a fatty liver present a hypoechoic mass within a fatty liver whatever the aetiology. However, with the aid an octreotide scan a tissue diagnosis of a carcinoid was achieved [2]*

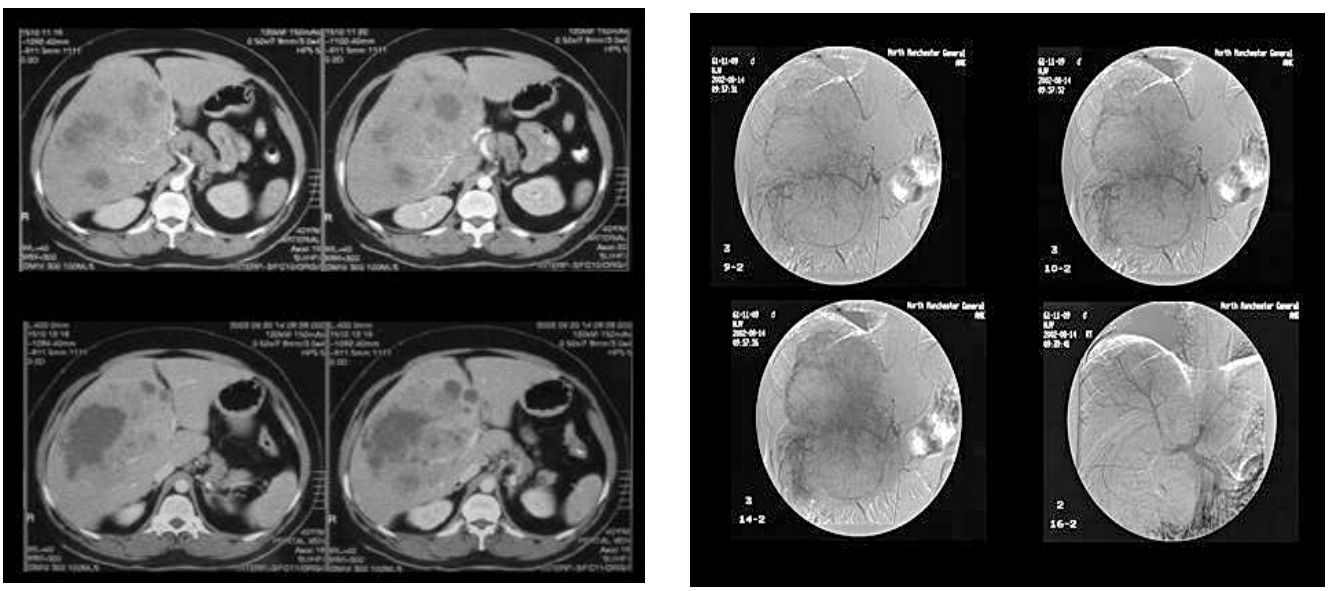

Figure 34 *Uptake of I-131 MIBG was more likely if neurohumor levels, particularly serum serotonin, were elevated. There was no relationship of I-131 MIBG uptake to carcinoid syndrome*

CEA immunoscintigraphy

CEA is a tumour-associated antigen arising from the entodermally derived epithelium of the GI tract. It is expressed in a variety of adenocarcinomas, such as bowel cancer. CEA is a self-antigen not recognized by the immune system as a foreign substance; therefore, it does not provoke an immune response. CEA occurs on the cell membrane of colorectal carcinomas. An anti-CEA antibody derived from a murine monoclonal Fab' fragment when labelled with ^{99m}Tc enables the imaging of CEA-expressing tumours. The technique may be refined by combining CEA immuno scintigraphy with CT.

A retrospective study on 31 patients with suspected recurrence of colon and ovarian carcinoma were assessed with OncoScint CR/OV immunoscintigraphy. The study revealed that OncoScint scintigraphy is a sensitive method for the identification of local recurrence and extra-hepatic metastases in colorectal and ovarian carcinoma. It also has an important role in the therapeutic decision-making process. In the liver, conventional imaging had a significantly higher detection rate than immunoscintigraphy (sensitivity 93% vs 28%) [78].

CEA is also expressed in inflammatory conditions such as Crohn disease; therefore, there is a potential for false-positive diagnoses. Activity in a normal liver, kidney, heart, and aorta also may lead to a false-positive diagnosis. The liver is the major site of normal uptake; therefore, detecting metastatic sites in the liver may be difficult. Colloid subtraction has been incorporated, but the results offer no great promise [79-80].

Monitoring Minimally Invasive therapies for liver tumours

Hansjörg Rempp and associates have recently reviewed the role of minimally invasive treatment for HCC including highly focused ultrasound, microwave ablation, and irreversible electroporation, and new aspects of radiofrequency ablation (RFA). RFA is reserved for patients with early-stage HCC with up to three lesions with a tumour diameter of ≤3 cm. The authors review the Indications and contraindications to treatment and compare the current image guided modalities. The options for treatment monitoring and intra-procedural tools and post-therapy imaging and functional parameters and control/prevention of local recurrence are discussed [81]. See figure 55.

Neuroendocrine & gastroenteropancreatic tumours

Neuroendocrine (NET) and gastroentero pancreatic tumours are rare neoplasms that often metastasize to the liver. Somatostatin-receptor scintigraphy is an essential component in the initial work up of NET for the detection of functioning metastases. Hepatic arterial embolization is often used to reduce liver tumour burden; alternatively laser treatment or RFA is used to de-bulk tumour burden. The medical treatment includes cytotoxic agents, alpha interferons and somatostatin analogues. To reduce clinical symptoms, somatostatin analogues are often combined with the other therapies. Chemotherapy is particularly useful in aggressive tumours with high proliferation capacity, whereas alpha interferon is useful in classical mid-gut carcinoids with low proli feration capacity. A recent innovation is somatostatin-based radioactive tumour targeted therapy. The preliminary results are promising, but larger studies are needed to determine its future role in the treatment of neuroendocrine tumours in patients [27].

Most GEP and NET tumours contain high-affinity binding sites for somatostatin, and as a result, somatostatin-receptor scintigraphy has evolved in the evaluation of these tumours. Ichijo et al. describe two patients, in whom it was quite difficult to localize GEP/NET tumours by conventional imaging techniques. The tumours were accurately localized by 111 In-DTPA-pentetreotide scintigraphy. In the first patient, multiple tumours were shown in the gastrinoma triangle, but it could not clarify whether there were any tumours in the pancreatic body. Selective arterial secretin injection test (SASI)

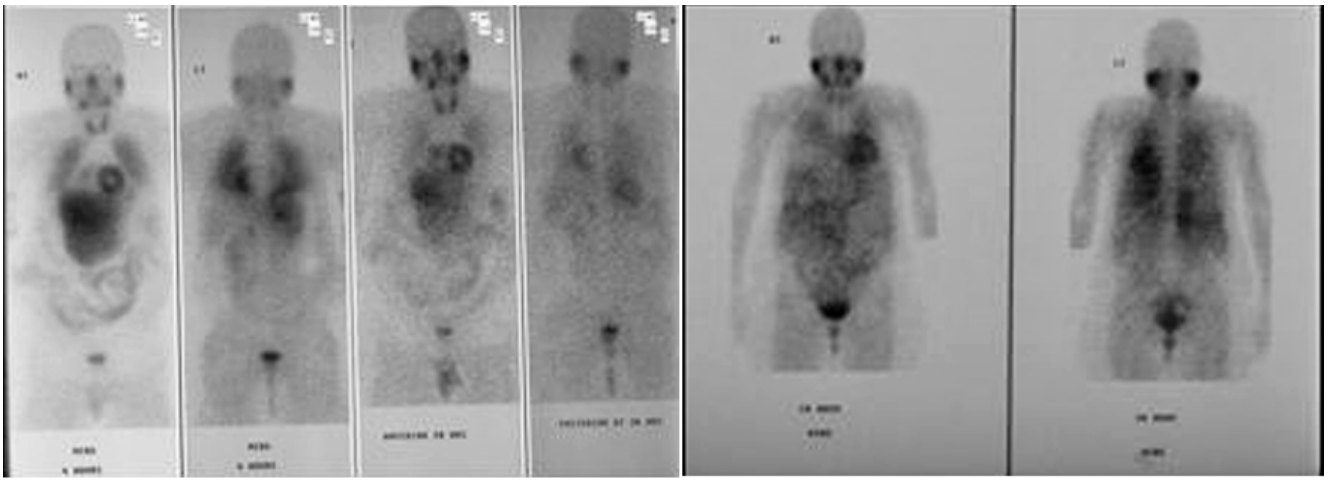

Figure 35 *Uptake of I-131 MIBG was more likely if neurohumor levels, particularly serum serotonin, were elevated. There was no relationship of I-131 MIBG uptake to carcinoid syndrome*

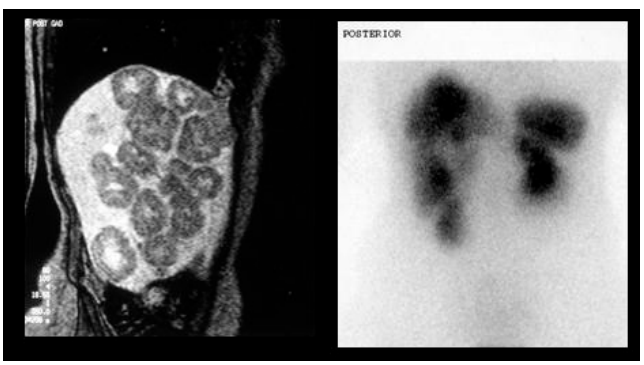

Figure 36 *Characteristic appearance of carcinoid liver metastases on planar indium-111 octreotide scan showing the primary lesion, mesenteric metastases, and multiple liver metastases*

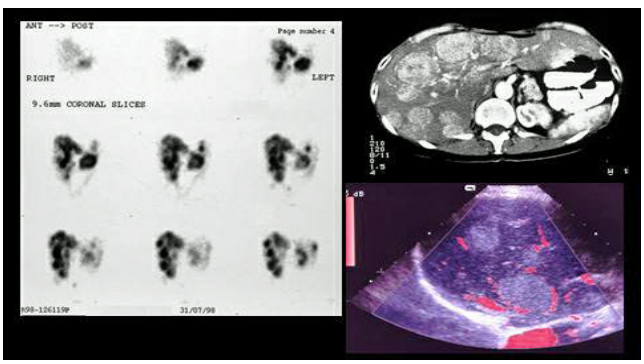

Figure 37 *Characteristic appearance of carcinoid liver metastases on contrast-enhanced axial CT scan showing early arterial enhancement of the liver metastases*

showed that the gastroduodenal artery was the feeder of the gastrinomas, and ^{111}In-DTPA-pentetreotide scintigraphy with single-photon emission computed tomography indicated the absence of tumours in the pancreatic body. In the second patient, with insulinoma, multiple liver tumours and a large mass in the hilum of the spleen were shown. ^{111}In-DTPA-pentetreotide scintigraphy was useful in determining that there was no secretion of insulin from the tumour in the hilum of the spleen. A CT scan is preferred for detection of NET as not all NETs have somatostatin receptors; however, somato statin receptor scanning, as well as the SASI test, may be useful for the surveillance of patients with known primary tumours, for monitoring patients with disseminated disease, and for following the treatment of these patients [30]. See Figures 47-50.

Stokkel *et al.* studied 88 consecutive patients with histologically confirmed well-differentiated NET. The aim of the study was to determine the value of somatostatin receptor scintigraphy (SRS) and Chromo granin A (CgA) assay in staging and follow-up

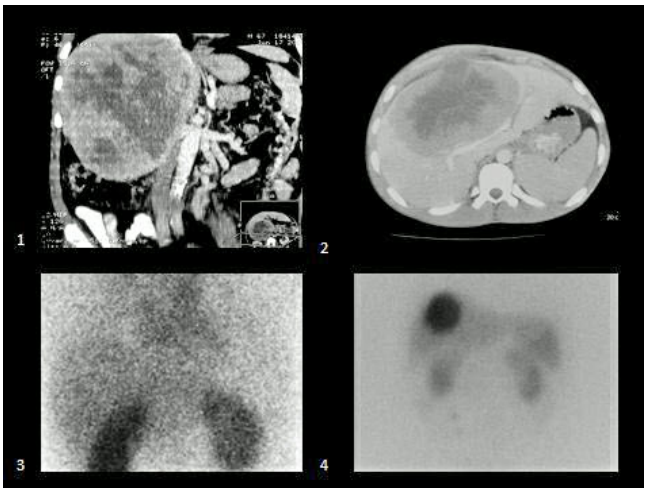

Figure 38 *This 40-year-old man presented with pyrexia and deranged liver function tests. The coronal CT reconstruction image (1) and axial CT image (2) show a large non-specific mass astride the left and right lobes compressing the left branch of the portal vein. The tumour shows central necrosis. A percutaneous biopsy was also non-diagnostic. Octreotide scans (3 & 4) show intense activity within the tumour. The final diagnosis was that of an intrahepatic carcinoid tumour*

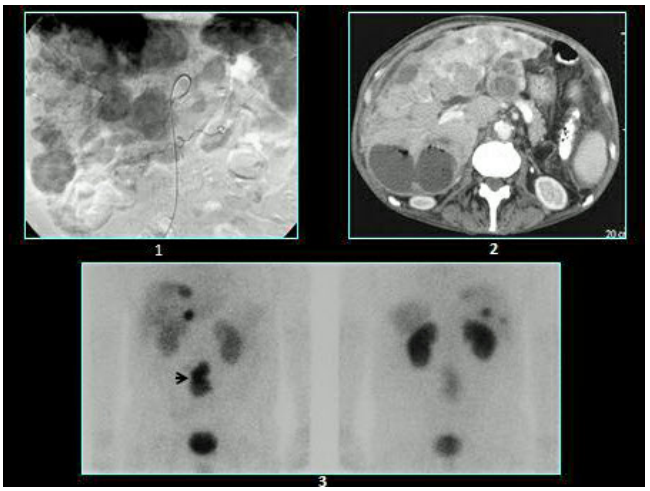

Figure 39 *Transcatheter embolization is a standard effective therapy for carcinoid metastases. Selective arteriography (1) shows extensive arterialised liver metastases. Post embolization CT scan show multiple necrotic metastases liver lesions, two with air within. It is difficult to ascertain as to how many of the liver tumours are viable. Post embolization octreotide scan (3) shows only remaining viable tumours. Note the primary bowel lesion showing intense activity (arrow)*

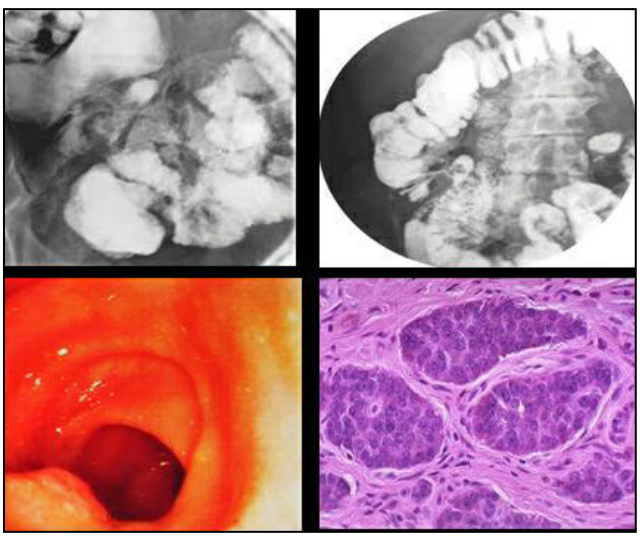

Figure 40 *Axial CT scans on the same patient as in Figure 42 shows the polypoid lesion in the terminal ileum (red arrow) with surrounding desmoplastic reaction and a metastatic deposit (black arrow). Also note small bowel dilatation*

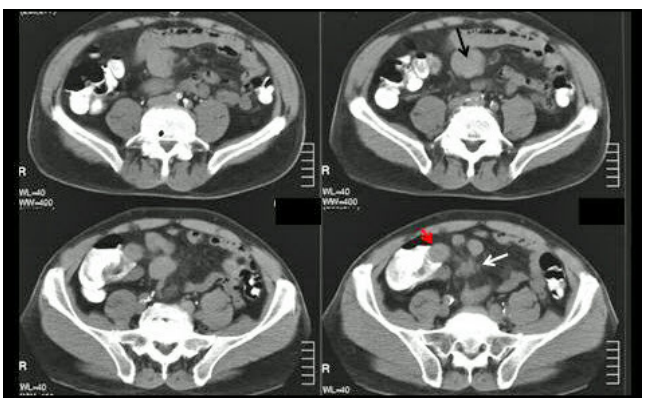

Figure 41 *This patient presented with abdominal pain. An upper GI series show a stricture at the terminal ileum and dilatation of the proximal bowel. At colonoscopy, a nodule was seen within the terminal ileum, which was biopsied. At high magnification, the nests of carcinoid tumor have a typical endocrine appearance with small round cells having small round nuclei and pink to pale blue cytoplasm were seen*

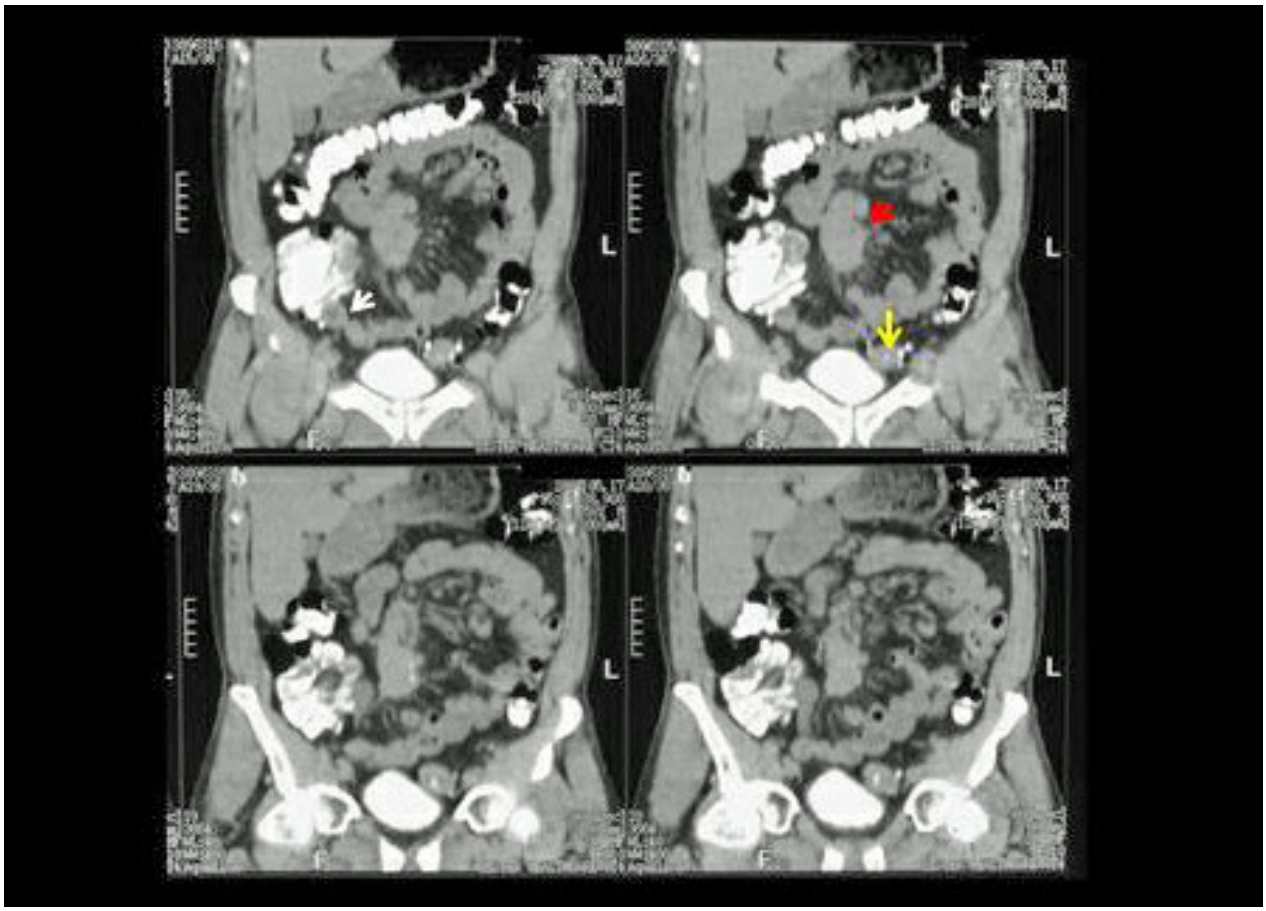

Figure 42 *Coronal reconstructed CT of the same patient as in Figures 43 shows the terminal ileum mass (white arrow), the mass in the epigastrium with surrounding desmoplastic reaction (red arrow) and a further mass adjacent to the urinary bladder (yellow arrow). All these signs contribute to the diagnosis but are not tissue-specific*

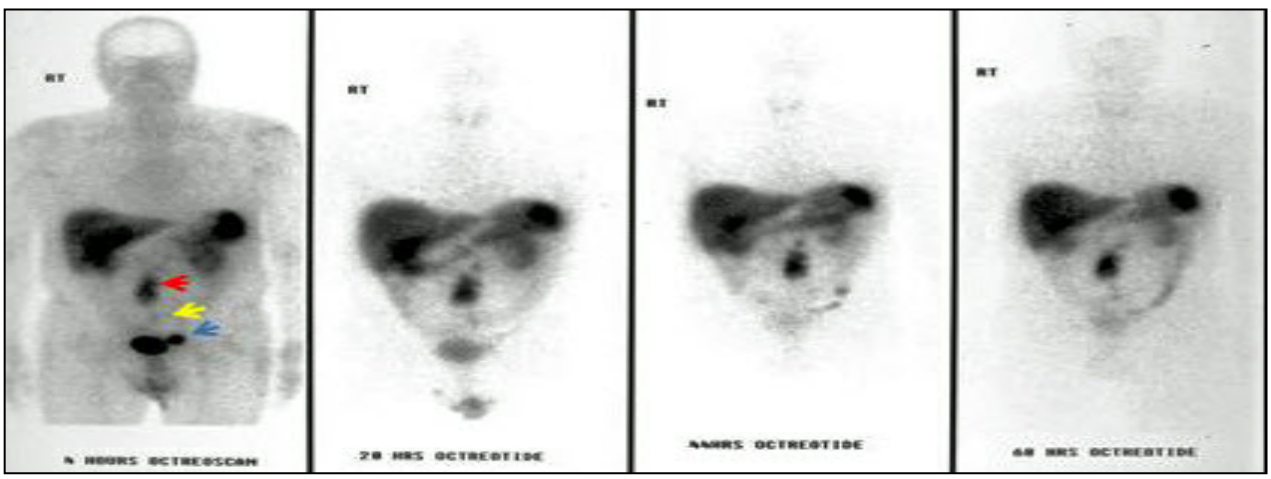

Figure 43 *Octreotide scan show faint activity at the site of the terminal ileum mass (yellow arrow), intense activity in the metastatic deposit (red arrow) and further activity adjacent to the urinary bladder (blue arrow)*

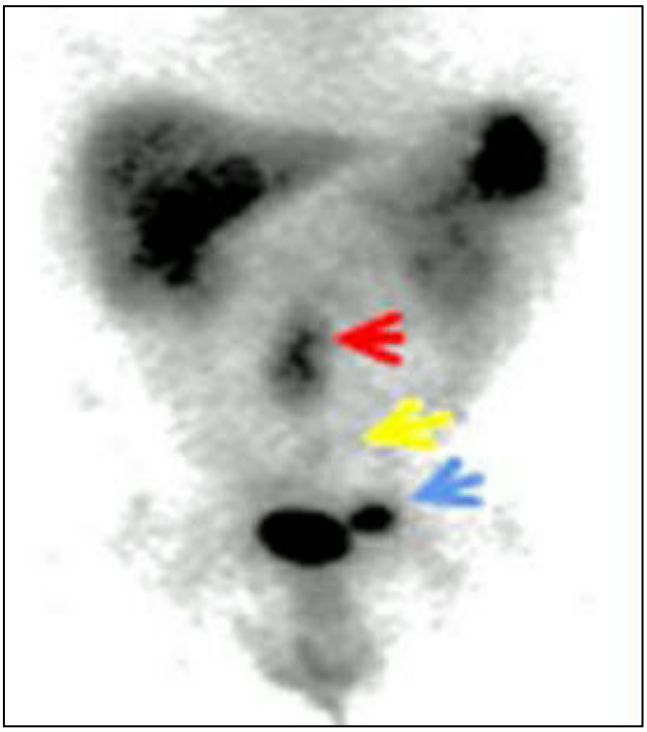

Figure 44 *Magnified view of figure 45 shows faint activity at the site of the terminal ileum mass (yellow arrow), intense activity in the metastatic deposit (red arrow) and further activity adjacent to the urinary bladder (blue arrow)*

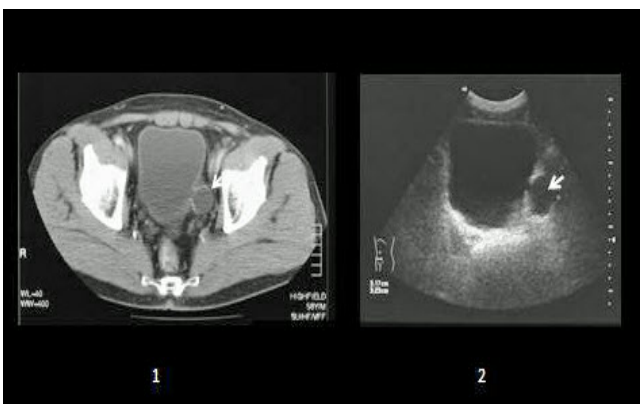

Figure 45 *Further interrogation of the images on the same patient as in Figures 42-44 show that the octreotide activity adjacent to the urinary bladder is within a bladder diverticulum. These images show the sensitivity of octreotide scans and the important contributory role of other imaging*

of patients with well-differentiated NETs. The study revealed that despite the higher sensitivity of SRS than of CgA in staging, and restaging well-differentiated NETs, both tests are required at the initial stage. Factors effecting SRS results and CgA values include disease extent, symptoms, and the presence of liver metastasis. CgA values were found a decisive factor in the assessment of tumour progression during follow-up, whereas the role of SRS in the routine follow-up of well-differentiated NETs was found to be limited [28].

Hepatic paragangliomas (ectopic pheochromo cytomas) are an extremely rare neoplasm that present with the non-specific appearance on CT and MRI. A non-functional primary hepatic paraganglioma in a 71- year old female' has been described for an octreotide scan supported diagnosis. This is a rare example where the role of nuclear medicine is crucial because it may help to determine future treatment in cases where there is suspicion of this tumour [29].

Calcitonin is a sensitive marker of medullary thyroid carcinoma (MTC). High concentrations of basal or pentagastrin stimulated calcitonin in patients with MTC is a signal of recurrence or metastatic disease. Detection of metastatic foci remains a diagnostic and therapeutic challenge. Diagnostic imaging early in the course of metastatic disease may be negative with US, CT MRI, scintigraphy, and ^{18}F-FDG-PET. However, recent case reports have shown that PET-CT scan with somatostatin analogue labelled with gallium (^{68}Ga-DOTA-TATE PET-CT) may be useful in the diagnostic imaging of patients with disseminated MTC [82].

In recent years, targeted therapies using radiolabeled compounds have emerged. Radiolabeled small molecules target receptors on tumour cells delivering high radiation doses to tumours in patients with disseminated disease. The role model of this approach is the development of radiolabeled somatostatin derivatives for the treatment of NETs. A number of radiopharmaceuticals are used in patients with inoperable hepatocellular carcinoma or liver metastases [31].

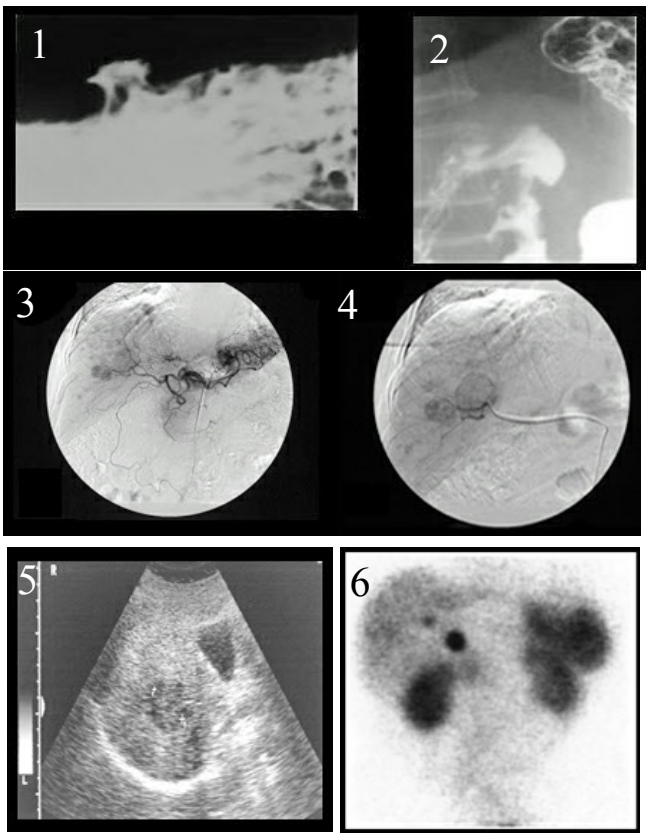

Figure 46 *Zollinger-Ellison Syndrome is caused by a non-beta islet cell, gastrin-secreting tumor of the pancreas that stimulates the acid-secreting cells of the stomach to maximal activity. Metastasis has a non-specific appearance on upper GI series, ultrasound (1, 2 & 3). The liver metastases arterially enhance on angiography (2 & 3) but still non-specific. Having said this appearance of gastric ulcer and pyloric canal ulcers on the GI series is suggestive but yet non-specific for Zollinger-Ellison Syndrome. Octreotide is a drug similar to somatostatin, is radiolabeled with indium-111. Tumours with somatostatin receptors are octreotide avid and show increased activity against a background of normal isotope uptake and thus providing tissue specific imaging in an appropriate clinical setting. Image 6 is an octreotide scan, which shows intense activity in the region of the tail of the pancreas and patchy activity in the liver secondary to liver metastases*

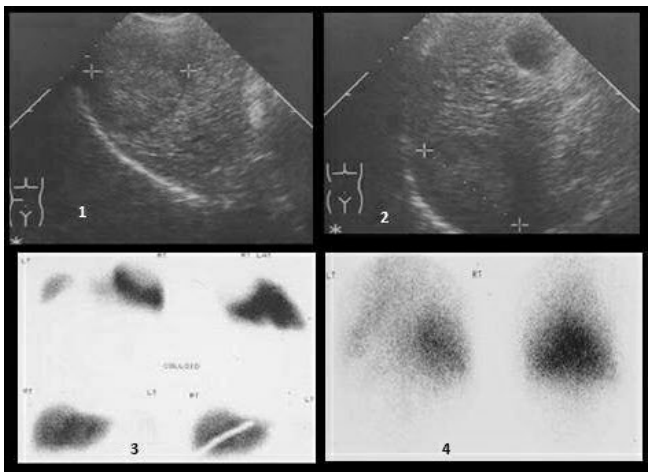

Figure 47 *Nuclear medicine was one of the earlier modality used to characterize HCC. The radionuclides used included ^{99m}Tc sulphur colloid, ^{67}Ga and ^{99m}Tc imino diacetate acid analogues. The images are from a patient that presented with non-specific symptoms. Ultrasound images (1 & 2) show a non-specific mass lesion within the liver. The colloid scan shows a photon deficient mass (3), the gallium-67 image (4) show uptake within the tumour. Surgery revealed a well-differentiated hepatocellular carcinoma*

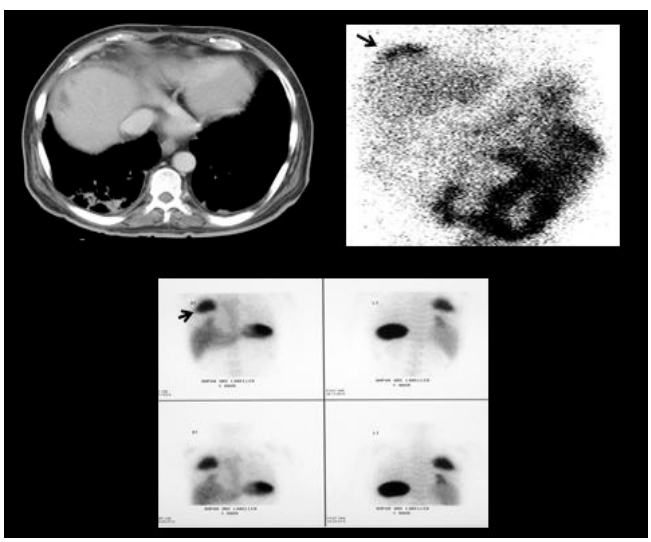

Figure 48 *Indium labelled WBC scan showing a subphrenic abscess in two separate patients. Note the axial CT scan show non-specific appearance*

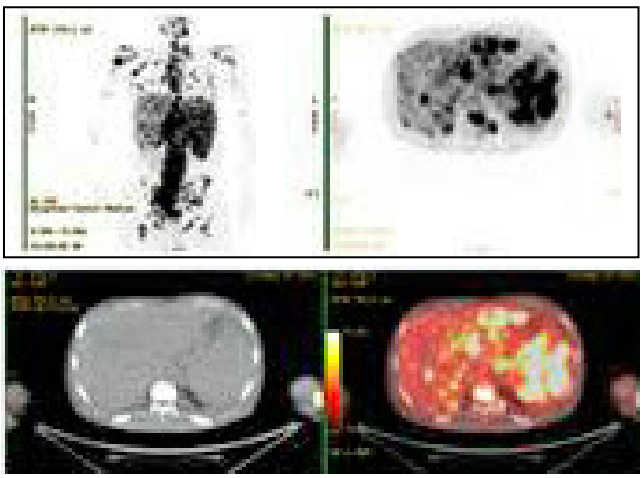

Figure 49 *FDG PET showing multiple lymphoma deposits in the liver, spleen and bone*

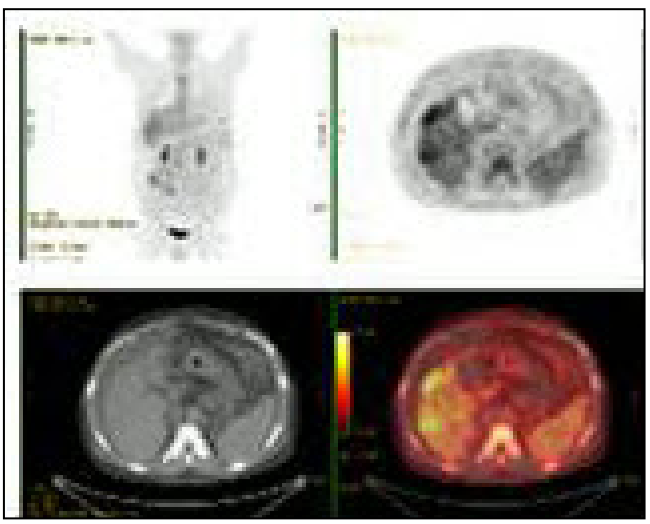

Figure 50 *Fluorine-18 fluorodeoxyglucose (FDG) positron emission tomography (PET) has proven record as a valuable tool in the initial diagnosis, staging, and restaging of many cancers. The sensitivity of FDG-PET in detecting HCC < or = 5 cm in size is low. However, for larger tumours, there is a strong correlation of sensitivity and uptake intensity with tumour size and elevated AFP levels. FDG-PET sensitivity and uptake intensity does not correlate with histologic grade. Whether FDG PET offers any benefit over traditional imaging has yet to be determined. Nevertheless, extrahepatic disease is depicted well on FDG-PET*

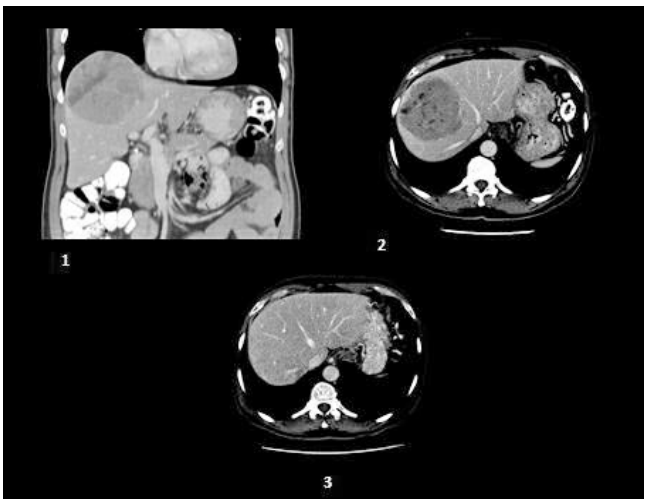

Figure 51 *Transcatheter chemoembol ization is an established treatment of inoperable hepatocellular carcinoma. Embolisation with Ytrium-90 TheraSphere is one of the options. TheraSphere consists of insoluble glass microspheres where yttrium-90 is an integral constituent of the glass. The images show a predominantly cystic HCC (1) and the result following two cycles (2 & 3) of Ytrium-90 TheraSpheres. Figure 1 after the first cycle show extensive tumour necrosis and figure 2 after the second cycle show only minor/subtle changes at the tumour site*

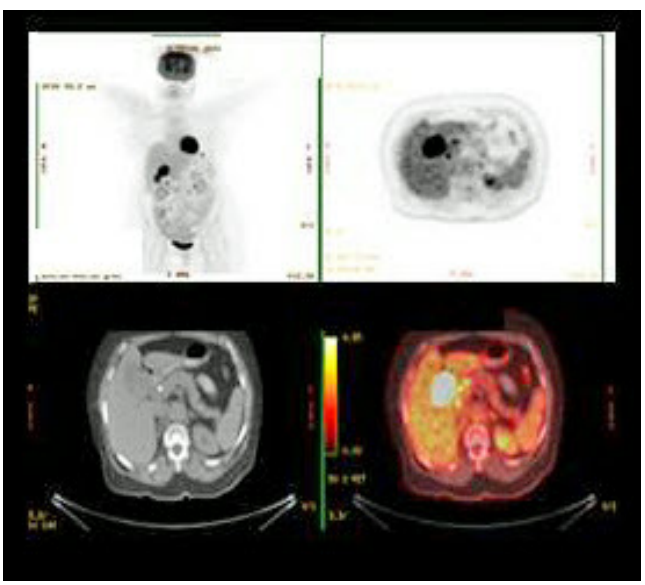

Figure 52 *FDG-PET showing liver metastases from carcinoma breast*

Diffuse liver disease

Hepatopulmonary syndrome

HPS is defined as a triad of liver disease, increased alveolar-arterial gradient while breathing room air, and evidence of intrapulmonary vascular dilatation [45]. HPS usually occurs in the setting of chronic liver disease. HPS can affect all ages and sometimes appear in non-cirrhotic patients with portal hypertension and has also been reported in mild liver disease [46]. The exact mechanism of HPS is not known but is most probably the result of variation in the production or clearance of chemical mediators causing intrapulmonary vascular vaso dilatation (IPVD) and significant AV shunting. A major drawback of IPVD is a ventilation-perfusion mismatch. Hypoxia occurs as a result of an inability of oxygen to diffuse through the markedly dilated peripheral lung vessels. These vessels are known to dilate 15-500 microns (n 8-15 microns) [51]. Imbalance in the endothelin receptor response, pulmonary microvascular remo delling and genetic predisposition is thought to lead to IPVD [83]. In children, HPS particularly occurs in cirrhotic portal hypertensive patients with severe hepatic dysfunction [54].

Imaging can depict ventilation-perfusion mismatch. A definitive diagnosis of HPS can be made by demonstrating of pulmonary vasodilatation with clear, functional shunting. This can be achieved by various means. Technetium-99m macroaggregated albumin (^{99m}Tc-MMA) perfusion imaging or contrast echocardiography (CEE). ^{99m}Tc-MMA perfusion scanning is a more sensitive method as it allows quantification of the amount of intrapulmonary shunting. ^{99m}Tc-MMA >20 microns in diameter are entrapped in pulmonary vasculature and sustain decay. In patients with a right to left shunt, the ^{99m}Tc-MMA enter the systemic circulation and is distributed to systemic organs. Normally, less than 5% of the isotope can be quantitated over the brain. In HPS, there is >6% uptake in the brain. A disadvantage of ^{99m}Tc-MMA is that it is unable to differentiate intracardiac from intrapulmonary shunt [48].

Perfusion Scintigraphy in HPS in children

El-Shabrawi *et al.* compared ^{99m}Tc-MAA perfusion lung scan to contrast enhanced echocardiography (CEE) in the diagnosis of HPS in children. The authors found ^{99m}Tc-MAA perfusion lung scan was more sensitive than CEE in diagnosis of intrapulmonary shunts. The SI cut off value of 0.278 was found to be highly specific for shunt detection [52].

Liver Functional Reserve

Shuke *et al.* examined data from 17 patients with liver cirrhosis and 3 patients with fatty liver, to compare the efficacy of 3 hepatic imaging agents in the evaluation of hepatic functional reserve. Evaluated here were ^{99m}Tc-galactosyl human serum albumin (GSA) which is a novel ligand for hepatic binding protein, ^{99m}Tc-N-pyridoxyl-5-methyl tryptophan (PMT) of a hepatobiliary agent, and ^{99m}Tc-Sn colloid. Using the data obtained the authors, analysed the correlations between the imaging agents used and the results of hepatic function tests. The data obtained from ^{99m}Tc-GSA imaging showed the most significant statistical association with the results of hepatic function tests. From this data, it was concluded that, ^{99m}Tc-GSA imaging provided the best assessment of hepatic functional reserve [43

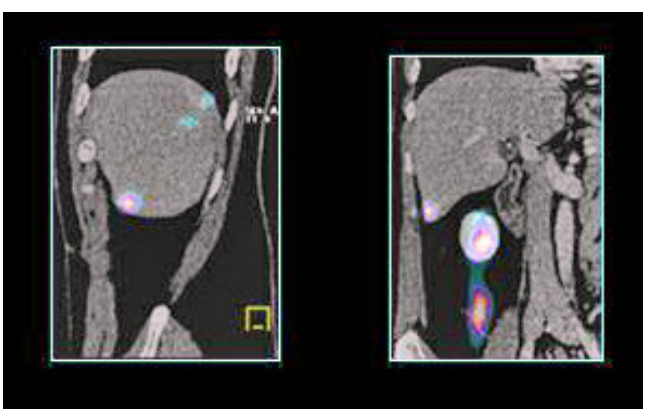

Figure 53 *FDG-PET images obtained by SPECT show multiple liver metastases*

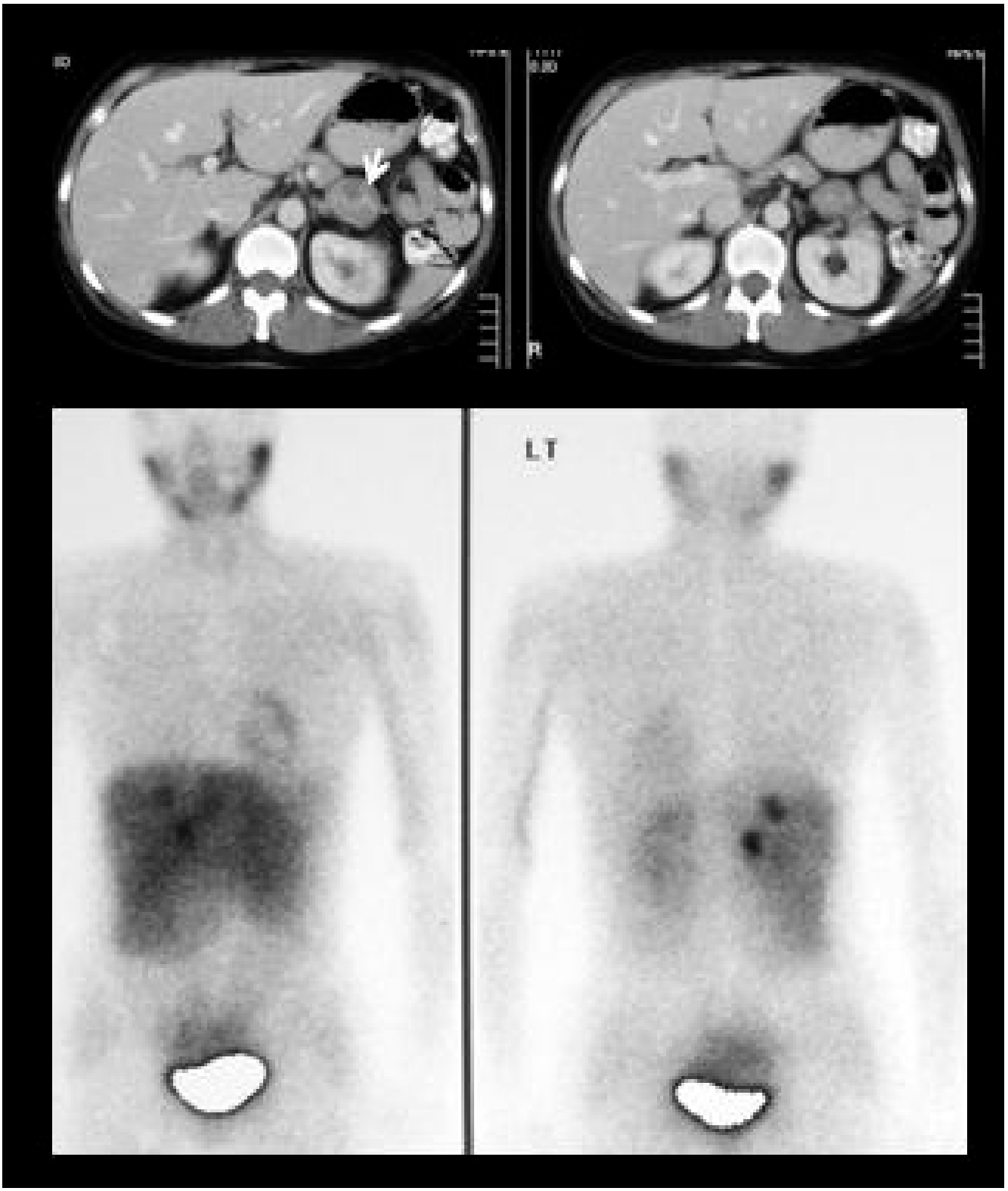

Figure 54 *MIBG uptake in pheochromocytoma and liver metastasis. The primary tumour was recognised on the CT (arrow) but the liver metastatic deposit is shown only by the MIBG scan*

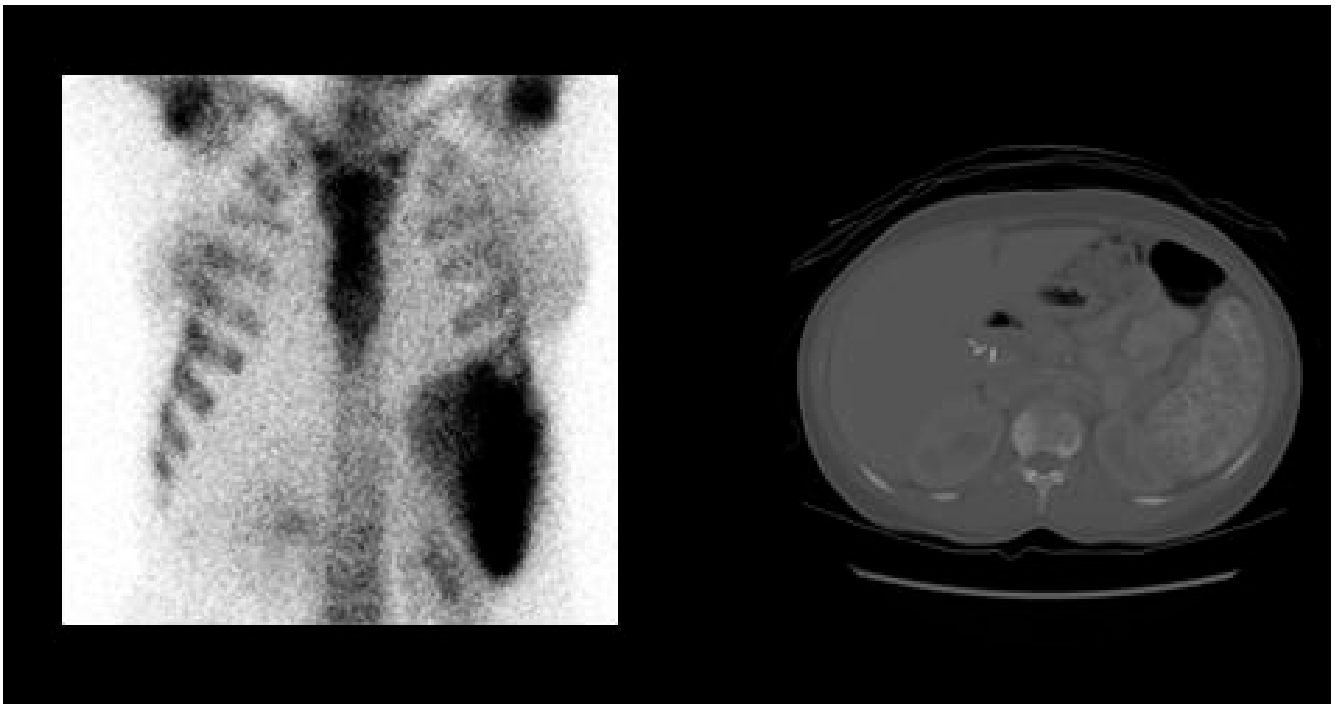

Figure 55 *This patient was being staged for carcinoma breast. There was intense uptake of 99mTc-Methyl diphosphonate within the spleen. The patient had history of Sickle cell disease. The CT scan shows calcification in the spleen due to autosplenectomy*

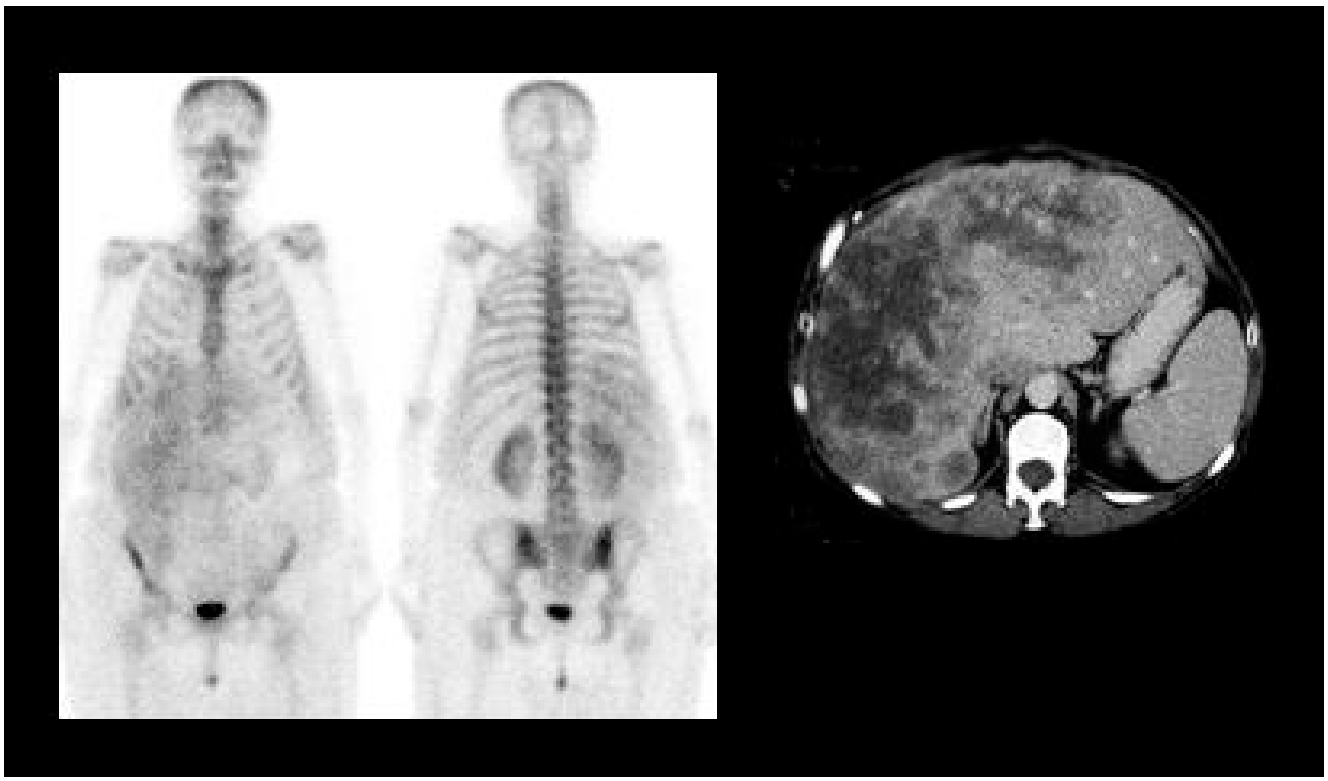

Figure 56 *FDG-PET showing liver metastases from carcinoma breast*

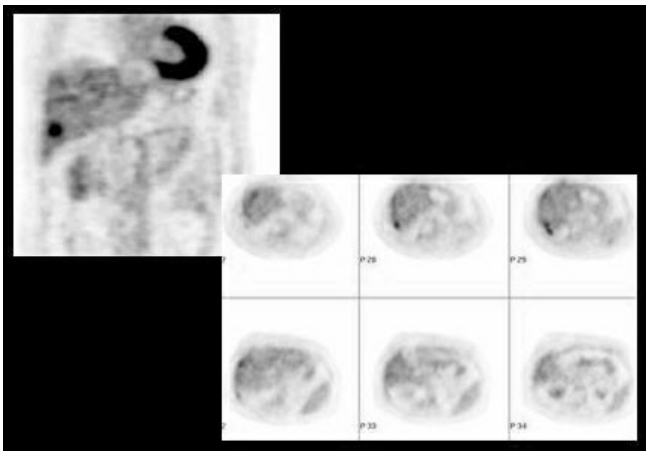

Figure 57 *FDG-PET showing colorectal metastases*

Portosystemic shunts in chronic liver disease

It is essential to assess both hepatic functional reserve and portal circulation in chronic liver disease. ^{99m}Tc-galactosyl human serum albumin scintigraphy, the index of blood clearance (HH15) and receptor index (LHL15) have been widely used in the evaluation hepatic functional reserve. Osada H et al. studied 82 patients with chronic liver disease in order to predict the prognosis and complications of the associated portal hypertension. The purpose of the study was to examine the relationship between HH15 and LHL15 and portosystemic shunts evaluated with arteriographic portography or oeso phagogastroduodenoscopy in chronic liver disease. The authors found HH15 a potent indicator of the presence of portosystemic shunts in chronic liver disease [84].

Cao *et al.* first reported hepatic radio embolization with Yttrium-90 glass microspheres for treatment of inoperable primary liver cancer. It is presently considered a worthwhile therapeutic approach because of encouraging rate of response or stabilization. Initial work up includes assessment of the degree of AV shunt before resorting to radioembolization. It is essential that intrapulmonary shunts are excluded by cross-sectional imaging. The same statement applies when dealing with HPS [85].

^{99m}Tc-MAA total-body imaging in right-to-left shunts

Detection of intrapulmonary left-to-right shunt is an essential prerequisite in various clinical scenarios including biliary atresia, radiolabelled chemoembolization for HCC and liver transplant candidates. The appearance of radiotracer in the systemic circulation to document the visualization of the brain, kidneys, and spleen after intravenous administration of ^{99m}Tc-MAA indicates right-to-left shunt because MAA particles (20-60 microns) are supposedly trapped in the pulmonary bed [47].

Evaluation of intrapulmonary shunt in normoxemic cirrhotic patients and effects of terlipressin

Intrapulmonary shunt (IPS) with hypoxemia is a feature of cirrhosis. However, the extent of intrapulmonary shunt (IPS) in cirrhotic patients without hypoxemia remains unclear. Kalambokis et al found that IPS fractions detected by ^{99m}Tc-MAA lung scan are inversely correlated with platelet count and directly with liver disease severity. The authors found IPS in 20% of normoxemic cirrhotic patients. In this study, treatment with Terlipressin was associated with a significant reduction in the magnitude of the IPS [53].

Per-rectal portal scintigraphy in liver disease

Shiomi *et al.* found Scintigraphy with ^{99m}Tc-diethylenetriaminepentaacetate with galacto syl human serum albumin (^{99m}Tc-GSA) and per-rectal portal scintigraphy useful for evaluating hepatic functional reserve and portal circulation, respectively. The authors recommend a combination of ^{99m}Tc-GSA per-rectal portal scintigraphy and ^{99m}Tc-pertechnetate for accurate assessment of the severity of chronic liver disease before treatment-making decisions because in some patients' the results are not correlated [50].

Preoperative pulmonary assessment of children for liver transplantation

Some observers believe that testing for HPS should be part of the preoperative study of paediatric patients with chronic liver disease undergoing liver transplantation, as it allows identification of pulmonary changes that can increase postoperative morbidity/mortality. The most common scintigraphic finding in HPS is heterogeneous pulmonary perfusion [49]. Scintigraphy with intravenous human albumin macroaggregates is more accurate than measuring arterial blood gases to detect IPS in children with cirrhosis [44].

Exploration of hepatic hydrothorax

Ajmi *et al.* reviewed 10 patients with cirrhosis associated hydrothorax to evaluate the performance of peritoneal scintigraphy in peritoneal-pleural communication and its role in therapeutic management. The study revealed peritoneal-pleural communication in nine patients. In four patients, radioactivity appeared in the pleural cavity within a few minutes after injection of the radiotracer. In three patients' ultrasonography, MRI or thoracoscopy revealed a large diaphragmatic defect. A full response to medical treatment was observed in four patients. Scintigraphy revealed rapid radioactivity migration in four patients; diuretic treatment led to resolution of the hydrothorax in one of them. Three patients refractory to medical treatment responded to talc pleurodesis. The authors found peritoneal scintigraphy a simple non-invasive technique to confirm a peritoneal-pleural communication in cirrhotic patients. More over a diaphragmatic deficiency can also be evaluated, providing a significant contribution to therapeutic decision-making [86].

Scintigraphic evaluation of TIPS

Transjugularly placed intrahepatic portocaval shunt (TIPS) dysfunction is usually assessed by Doppler sonography although angiography remains the gold standard. However, there is an on-going search for non-invasive techniques, for the early detection of shunt insufficiency. Liver perfusion scintigraphy with technetium-99m diethylene triamine penta-acetic acid can detect changes in the hepatic blood flow after TIPS shunting. Scintigraphy prior to TIPS shows that the portal venous contribution to hepatic perfusion is reduced to 29.2% this decrease is due to portal hypertension. Following TIPS procedure there is a significant increase in portal venous perfusion. TIPS shunt occlusion is identified in patients by a significant reduction in the scintigraphically measured portal venous contribution to hepatic blood flow. Hepatic perfusion scintigraphy demonstrates the immediate consequence of TIPS on hepatic blood flow. Post-TIPS follow-up studies of hepatic haemodynamics by liver perfusion scintigraphy seem able to contribute to the detection of TIPS shunt occlusion before the clinical consequences are obvious [87-88]. A variety of other applications are presented in the images (Figures 50-57).

Conclusion

Recent decades have seen replacement of many liver scintigraphic studies by cross sectional imaging. However, liver scintigraphy has emerged stronger with the advent of many, innovations in new radionuclides and the emergence of PET/CT and SPECT. Liver scintigraphy has moved into more tissue specific imaging and into areas where it provides more superior imaging than cross sectional imaging.

References

1. Duman DG, Dede F, Akin H, Sen F, Turo?lu HT, Celikel C, Tözün N. Colloid scintigraphy in non-alcoholic steatohepatitis: a conventional diagnostic method for an emerging disease. Nucl Med Commun. 2006Apr;27(4):387-93.
2. Caglar M, Sari O, Akcan Y. Prediction of therapy response to interferon-alpha in chronic viral hepatitis-B by liver and hepatobiliary scintigraphy. Ann Nucl Med. 2002 Nov;16(7):511-4.

3. Massey MD, Stevens JS. Residual spleen found on denatured red blood cell scan following negative colloid scans. J Nucl Med. 1991 Dec;32(12):2286-7.

4. Mortelé KJ, Mortelé B, Silverman SG. CT features of the accessory spleen. AJR Am J Roentgenol. 2004;183 (6): 1653-7. Invest Radiol. 1986 Jan;21(1):1-11.

5. Guze BH, Hawkins R.The utility of SPECT liver-spleen imaging in the evaluation of a possible accessory spleen. Clin Nucl Med. 1988 Jul;13(7):496-7.

6. Weiand G, Mangold G.[Accessory spleen in the pancreatic tail -- a neglected entity? A contribution to embryology, topography and pathology of ectopic splenic tissue]. Chirurg. 2003 Dec;74(12):1170-7. [Article in German]

7. Läuffer JM, Baer HU, Maurer CA, Wagner M, Zimmermann A, Büchler MW. Intrapancreatic accessory spleen. A rare cause of a pancreatic mass. Int J Pancreatol. 1999 Feb;25(1):65-8.

8. Belkhir SM, Archambaud F, Prigent A, Chaumet-Riffaud P. Intrapancreatic accessory spleen diagnosed on radionuclide imaging. Clin Nucl Med. 2009 Sep;34(9):642-4.

9. Zhang Z, Wang JC. An epithelial splenic cyst in an intrapancreatic accessory spleen. A case report. JOP. 2009 Nov 5;10(6):664-6.

10. Noel A, Harbert JC. Splenic simulation by left hepatic lobe following splenectomy Clin Nucl Med. 1984 Mar;9(3):147-8.

11. Person RE, Bender JM. Hepatic lesion differentiated from accessory spleen by a heat-damaged red blood cell scan. Clin Nucl Med. 2000 Jul;25(7):516-8.

12. MacDonald JK, Wilke RA, Jacobs WE. Accessory spleens in the thoracic and abdominal cavities after a relapse of idiopathic thrombocytopenic purpura: a case report. J Nucl Med Technol. 2000 Mar;28(1):49-51.

13. Stein S, Duarte PS, Alavi A, Zhuang H, Alavi JB. Multiple intraabdominal soft-tissue masses in a man awaiting liver transplantation: a case study and discussion. Am J Clin Oncol. 2000 Oct;23(5):506-8.

14. Rosenblatt GS, Luthringer DJ, Fuchs GJ. Enlargement of accessory spleen after splenectomy can mimic a solitary adrenal tumour. Urology. 2010 Mar;75(3):561-2. Epub 2009 Aug 13.

15. Chin S, Isomoto H, Mizuta Y, Wen CY, Shikuwa S, Kohno S. Enlarged accessory spleen presenting stomach submucosal tumour. World J Gastroenterol. 2007 Mar 21;13(11):1752-4.

16. Ota T, Kusaka S, Mizuno M. A splenic pseudotumour: an accessory spleen. Ann Nucl Med. 2003 Apr;17(2):159-60.

17. Antevil J, Thoman D, Taller J, Biondi M. Laparoscopic accessory splenectomy with intraoperative gamma probe localization for recurrent idiopathic thrombocytopenic purpura. Surg Laparosc Endosc Percutan Tech. 2002 Oct;12(5):371-4.

18. Hendrickson RJ, Koniaris LG, Kovach SJ, Johnson JA. Gamma probe-confirmed laparoscopic accessory splenectomy. Surg Endosc. 2002 Sep;16(9):1364.

19. Borse R, Mahapatra GN, Meht R, Plumber S, Dhuri S, Ali S. Scintigraphic finding of a silent hepatic haemangioma. J Assoc Physicians India. 2010 Oct;58:637-40.

20. Al-Hawary MM, Haddad MC, Hourani MH, Birjawi GA, Al-Kutoubi AO. Imaging of common benign solid liver tumours. J Med Liban. 2002 Sep-Dec;50(5-6):237-46.

21. Kume N, Suga K, Nishigauchi K, Shimizu K, Matsunaga N. Characterization of hepatic adenoma with atypical appearance on CT and MRI by radionuclide imaging. Clin Nucl Med. 1997 Dec;22(12):825-31.

22. Lisbona R, Mishkin S, Derbekyan V, Novales-Diaz JA, Roy A, Sanders L. Role of scintigraphy in focally abnormal sonograms of fatty livers. J Nucl Med. 1988 Jun;29(6):1050-6.

23. Buck AK, Herrmann K, Eckel F, Beer AJ.

Pancreatic and hepatobiliary cancers. Methods Mol Biol. 2011;727:243-64.

24. Maffioli L, Mascheroni L, Mongioj V, Gasparini M, Baldini MT, Seregni E, Castellani MR, Cascinelli N, Buraggi GL. Scintigraphic detection of melanoma metastases with a radiolabeled benzamide ([iodine-123]-(S)-IBZM). J Nucl Med. 1994 Nov;35(11):1741-7.
25. Bernard EJ, Nicholls W, Howman-Giles R, Kan A, Stevens M. Tl-201 positive, Ga-67 negative hepatoblastoma: a case report of a 12-year-old boy. Clin Nucl Med. 1997 Dec;22(12):835-7.
26. Gharib AM, Thomasson D, Li KC Molecular imaging of hepatocellular carcinoma. Gastroenterology. 2004 Nov;127(5 Suppl 1):S153-8.
27. Oberg K. State of the art and future prospects in the management of neuroendocrine tumours. Q J Nucl Med. 2000 Mar;44(1):3-12.
28. Stokkel MP, Rietbergen DD, Korse CM, Taal BG. omatostatin receptor scintigraphy and chromogranin A assay in staging and follow-up of patients with well-differentiated neuroendocrine tumours. Nucl Med Commun. 2011 Aug;32(8):731-7.
29. Antontiou D, Papatheodorou H, Ziras N, Zizi-Serbetzoglou A, Paschalidis N, Christopoulou A, Filippakou E, Trivizaki E. Hell J Nucl Med. 2011 May-Aug;14(2):163-5. Radioisotopic and anatomical imaging approach of a primary non functioning liver paraganglioma.
30. Ichijo T, Ishikawa M, Shimojo M, Tsubuku M, Tsuboi K, Miyachi Y. Role of (111)In-DTPA-pentetreotide scintigraphy in accurate diagnosis of neuroendocrine gastroenteropancreatic tumours. J Hepatobiliary Pancreat Surg. 2001;8(5):473-8.
31. Oyen WJ, Bodei L, Giammarile F, Maecke HR, Tennvall J, Luster M, Brans B. Targeted therapy in nuclear medicine--current status and future prospects. Ann Oncol. 2007 Nov;18(11):1782-92. Epub 2007 Apr 13.
32. Huffman JL, Schenker S. Acute acalculous cholecystitis: a review. Clin Gastroenterol Hepatol. 2010 Jan;8(1):15-22. Epub 2009 Sep 10.
33. Fleming KW, Lucey BC, Soto JA, Oates ME. Posttraumatic bile leaks: role of diagnostic imaging and impact on patient outcome. Emerg Radiol. 2006 Mar;12(3):103-7. Epub 2005 Dec 21.
34. Mittal BR, Sunil HV, Bhattacharya A, Singh B Hepatobiliary scintigraphy in management of bile leaks in patients with blunt abdominal trauma. ANZ J Surg. 2008 Jul;78(7):597-600.
35. Balakrishnan VB, Kumar R, Dhanpathi H, Nadig M, Mohapatra T, Bal CS, Malhotra A.Hepatobiliary scintigraphy in detecting lesser sac bile leak in postcholecystectomy patients: need to recognize as a separate entity. Clin Nucl Med. 2008 Mar;33(3):161-7
36. Tripathi M, Chandrashekar N, Kumar R, Thomas EJ, Agarwal S, Bal CS, Malhotra A.Hepatobiliary scintigraphy. An effective tool in the management of bile leak following laparoscopic cholecystectomy. Clin Imaging. 2004 Jan-Feb;28(1):40-3.
37. Al Sofayan MS, Ibrahim A, Helmy A, Al Saghier MI, Al Sebayel MI, Abozied MM. Nuclear imaging of the liver: is there a diagnostic role of HIDA in posttransplantation? Transplant Proc. 2009 Jan-Feb;41(1):201-7.
38. Gencoglu EA, Kocabas B, Moray G, Aktas A, Karakayali H, Haberal M. Usefulness of hepatobiliary scintigraphy for the evaluation of living related liver transplant recipients in the early postoperative period. Transplant Proc. 2008 Jan-Feb;40(1):234-7.
39. Young SA, Sfakianakis GN, Pyrsopoulos N, Nishida S. Hepatobiliary scintigraphy in liver transplant patients: the "blind end sign" and its differentiation from bile leak. Clin Nucl Med. 2003 Aug;28(8):638-42.

40. Kula M, Karacavus S, Baskol M, Deniz K, Abdulrezzak U, Tutus A. Hepatobiliary function assessed by 99mTc-mebrofenin cholescintigraphy in the evaluation of fibrosis in chronic hepatitis: histopathological correlation. Nucl Med Commun. 2010 Apr;31(4):280-5.

41. Madácsy L, Middelfart HV, Matzen P, Hojgaard L, Funch-Jensen P Quantitative hepatobiliary scintigraphy and endoscopic sphincter of Oddi manometry in patients with suspected sphincter of Oddi dysfunction: assessment of flow-pressure relationship in the biliary tract. Eur J Gastroenterol Hepatol. 2000 Jul;12(7):777-86.

42. Vanagas T, Gulbinas A, Pundzius J, Barauskas G. Radiofrequency ablation of liver tumours (II): clinical application and outcomes. Medicina (Kaunas). 2010;46(2):81-8.

43. Shuke N, Aburano T, Nakajima K, Yokoyama K, Sun BF, Matsuda H, Muramori A, Michigishi T, Tonami N, Hisada K, et al. [The utility of quantitative 99mTc-GSA liver scintigraphy in the evaluation of hepatic functional reserve: comparison with 99mTc-PMT and 99mTc-Sn colloid]. Kaku Igaku. 1992 May;29(5):573-84. [Article in Japanese]

44. Grimon G, André L, Bernard O, Raffestin B, Desgrez A. Early radionuclide detection of intrapulmonary shunts in children with liver disease. J Nucl Med. 1994 Aug;35(8):1328-32.

45. Krowka MJ, Cortese DA. Hepatopulmonary syndrome: current concepts in diagnostic and therapeutic considerations. Chest 1994; 105:1528-1537.

46. Abrams GA, Jaffe CC, Hoffer PB, et al. Diagnostic utility of contrast echocardiography and lung perfusion scan in patients with hepatopulmonary syndrome. Gastroenterology. 1995;109:1283-8.

47. Lu G, Shih WJ, Chou C, Xu JY. Tc-99m MAA total-body imaging to detect intrapulmonary right-to-left shunts and to evaluate the therapeutic effect in pulmonary arteriovenous shunts. Clin Nucl Med. 1996 Mar;21(3):197-202.

48. McAdams HP, Erasmus J, Crockett R, Mitchell J, Godwin JD, McDermott VG. The hepatopulmonary syndrome: radiologic findings in 10 patients. AJR Am J Roentgenol 1996; 166:1379-1385.

49. Alves L, Sant'Anna CC, March Mde F, Ferreira S, Marsillac M, Tura M, O?ate H. Preoperative pulmonary assessment of children for liver transplantation. Pediatr Transplant. 2008 Aug;12(5):536-40. Epub 2008 Jan 8.

50. Shiomi S, Iwata Y, Sasaki N, Kurooka H, Tamori A, Habu D, Takeda T, Nishiguchi S, Kuroki T, Ochi H. Clinical need for both scintigraphy with technetium-99m GSA and per-rectal portal scintigraphy in some patients with chronic liver disease. Ann Nucl Med. 1999 Aug;13(4):241-5

51. Castro M, Krowka MJ. Hepatopulmonary syndrome: a pulmonary vascular complication of liver disease. Clin Chest Med 1996; 17:35-48. de Mac?do LG, Lopes EP Hepatopulmonary syndrome: an update. Sao Paulo Med J. 2009 Jul;127(4):223-30.

52. El-Shabrawi MH, Omran S, Wageeh S, Isa M, Okasha S, Mohsen NA, Zekry O, E-Bartan G, El-Karaksy HM. (99m)Technetium-macroaggregated albumin perfusion lung scan versus contrast enhanced echocardiography in the diagnosis of the hepatopulmonary syndrome in children with chronic liver disease. Eur J Gastroenterol Hepatol. 2010 Aug;22(8):1006-12.

53. Kalambokis G, Baltayiannis G, Tsiouris S, Pappas K, Kokkinou P, Fotopoulos A, Tsianos EV. Scintigraphic evaluation of intrapulmonary shunt in normoxemic cirrhotic patients and effects of terlipressin. Hepatol Res. 2010 Oct;40(10):1015-21.

54. Sari S, Oguz D, Sucak T, Dalgic B, Atasever T. Hepatopulmonary Syndrome in Children with Cirrhotic and Non-Cirrhotic Portal Hypertension: A Single-Center Experience. Dig Dis Sci. 2011 Jul 27. [Epub ahead of print]

55. Cheung TT, Chan SC, Ho CL, Chok KS, Chan AC, Sharr WW, Ng KK, Poon RT, Lo CM, Fan ST.Can positron emission tomography with the dual tracers [11 C]acetate and [18 F]fludeoxyglucose predict microvascular invasion in hepatocellular carcinoma? Liver Transpl. 2011 Oct;17(10):1218-25.

56. Dodd GD 3rd, Baron RL, Oliver JH 3rd, Federle MP. Spectrum of imaging findings of the liver in end-stage cirrhosis: part II, focal abnormalities. AJR Am J Roentgenol. Nov 1999;173(5):1185-92

57. el-Desouki M, Mohamadiyeh M, al-Rashed R, Othman S, al-Mofleh I. Features of hepatic cavernous hemangioma on planar and SPECT Tc-99m-labeled red blood cell scintigraphy. Clin Nucl Med. Aug 1999;24(8):583-9.

58. Craig JR, Peters RL, Edmondson HA, Omata M. Fibrolamellar carcinoma of the liver: a tumour of adolescents and young adults with distinctive clinico-pathologic features. Cancer. Jul 15 1980;46(2):372-9.

59. Wanless IR, Albrecht S, Bilbao J, Frei JV, Heathcote EJ, Roberts EA. Multiple focal nodular hyperplasia of the liver associated with vascular malformations of various organs and neoplasia of the brain: a new syndrome. Mod Pathol. Sep 1989;2(5):456-62.

60. Knowles DM 2nd, Casarella WJ, Johnson PM, Wolff M. The clinical, radiologic, and pathologic characterization of benign hepatic neoplasms. Alleged association with oral contraceptives. Medicine (Baltimore). May 1978;57(3):223-37.

61. Carlson SK, Johnson CD, Bender CE, Welch TJ. CT of focal nodular hyperplasia of the liver. AJR Am J Roentgenol. Mar 2000;174(3):705-12.

62. Kubaska S, Sahani DV, Saini S, et al. Dual contrast enhanced magnetic resonance imaging of the liver with superparamagnetic iron oxide followed by gadolinium for lesion detection and characterization. Clin Radiol. May 2001;56(5):410-5. [Medline].

63. Dähnert W. Disorders of liver, biliary tract and spleen. In: Radiology Review Manual. 6th Edition. Philadelphia, Pa: Wolters Kluwer Health; 2006:714-715.

64. Finlay IG, Meek DR, Gray HW, Duncan JG, McArdle CS. Incidence and detection of occult hepatic metastases in colorectal carcinoma. Br Med J (Clin Res Ed). 1982 Mar 13;284(6318):803-5

65. Leen E.The detection of occult liver metastases of colorectal carcinoma. J Hepatobiliary Pancreat Surg. 1999;6(1):7-15.

66. Drane WE. Nuclear medicine techniques for the liver and biliary system. Update for the 1990s. Radiol Clin North Am. Nov 1991;29(6):1129-50.

67. Dragoteanu M, Cotul SO, Pîgleşan C, Tamaş S. Liver angioscintigraphy: clinical applications. Rom J Gastroenterol. 2004 Mar;13(1):55-63.

68. Arulampalam T, Costa D, Visvikis D. The impact of FDG-PET on the management algorithm for recurrent colorectal cancer. Eur J Nucl Med. Dec 2001;28(12):1758-65.

69. Rohren EM, Paulson EK, Hagge R, Wong TZ, Killius J, Clavien PA. The role of F-18 FDG positron emission tomography in preoperative assessment of the liver in patients being considered for curative resection of hepatic metastases from colorectal cancer. Clin Nucl Med. Aug 2002;27(8):550-5.

70. Sacks A, Peller PJ, Surasi DS, Chatburn L, Mercier G, Subramaniam RM. Value of PET/CT in the management of liver metastases, part 1. AJR Am J Roentgenol. 2011 Aug;197(2):W256-9.

71. Patel S, McCall M, Ohinmaa A, Bigam D, Dryden DM. Positron emission tomography/computed tomographic scans compared to computed tomographic scans for detecting colorectal liver metastases: a systematic review. Ann Surg. 2011 Apr;253(4):666-71.

72. Maas M, Rutten IJ, Nelemans PJ, Lambregts DM, Cappendijk VC, Beets GL, Beets-Tan RG. What is the most accurate whole-body imaging modality for assessment of local and distant recurrent disease in colorectal cancer? A meta-analysis : imaging for recurrent colorectal cancer. Eur J Nucl Med Mol Imaging. 2011 Aug;38(8):1560-71. Epub 2011 Apr 6.

73. Niekel MC, Bipat S, Stoker J. Diagnostic imaging of colorectal liver metastases with CT, MR imaging, FDG PET, and/or FDG PET/CT: a meta-analysis of prospective studies including patients who have not previously undergone treatment. Radiology. 2010 Dec;257(3):674-84. Epub 2010 Sep 9.

74. Ruers TJ, Wiering B, van der Sijp JR, Roumen RM, de Jong KP, Comans EF, Pruim J, Dekker HM, Krabbe PF, Oyen WJ. Improved selection of patients for hepatic surgery of colorectal liver metastases with (18)F-FDG PET: a randomized study. J Nucl Med. 2009 Jul;50(7):1036-41. Epub 2009 Jun 12.

75. Jager PL, Chirakal R, Marriott CJ, Brouwers AH, Koopmans KP, Gulenchyn KY. 6-L-18F-fluorodihydroxyphenylalanine PET in neuroendocrine tumours: basic aspects and emerging clinical applications. J Nucl Med. 2008 Apr;49(4):573-86. Epub 2008 Mar 14.

76. Koopmans KP, de Vries EG, Kema IP, Elsinga PH, Neels OC, Sluiter WJ, van der Horst-Schrivers AN, Jager PL. Staging of carcinoid tumours with 18F-DOPA PET: a prospective, diagnostic accuracy study. Lancet Oncol. 2006 Sep;7(9):728-34.

77. Adalet I, Koçak M, Og?z H, Alagöl F, Cantez S. Determination of medullary thyroid carcinoma metastases by 201Tl, 99Tcm(V)DMSA, 99Tcm-MIBI and 99Tcm-tetrofosmin. Nucl Med Commun. 1999 Apr;20(4):353-9.

78. Pinkas L, Robins PD, Forstrom LA, Mahoney DW, Mullan BP. Clinical experience with radiolabelled monoclonal antibodies in the detection of colorectal and ovarian carcinoma recurrence and review of the literature. Nucl Med Commun. 1999 Aug;20(8):689-96.

79. Fuster D, Maurel J, Muxí A, Setoain X, Ayuso C, Martín F, Ortega ML, Fuertes S, Pons F. Is there a role for (99m)Tc-anti-CEA monoclonal antibody imaging in the diagnosis of recurrent colorectal carcinoma? Q J Nucl Med. 2003 Jun;47(2):109-15.

80. Artiko V, Petrović M, Sobić-Saranović D, Antić A, Koljević-Marković A, Krajnović-Jaksić E, Saranović D, Petrović N, Stojković M, Durutović D, Zuvela M, Radovanović-Bobić A, Galun D, Petrasinović Z, Pavlović S, Krivokapić Z, Obradović V. Radioimmunoscintigraphy of colorectal carcinomas with 99mTc-labelled antibodies. Hepatogastroenterology. 2011 Mar-Apr;58(106):347-51.

81. Hansjörg Rempp, Andreas Boss, Thomas Helmberger and Philippe Pereira The current role of minimally invasive therapies in the management of liver tumours Abdominal Imaging Volume 36, Number 6, 635-647, DOI: 10.1007/s00261-011-9749-2

82. Pałyga I, Kowalska A, Gąsior-Perczak D, Tarnawska-Pierścińska M, Słuszniak J, Sygut J, Góźdź S. The role of PET-CT scan with somatostatin analogue labelled with gallium-68 (??Ga-DOTA-TATE PET-CT) in diagnosing patients with disseminated medullary thyroid carcinoma (MTC). Endokrynol Pol. 2010 Sep-Oct;61(5):507-11

83. Mac?do LG, Lopes EP. Hepatopulmonary syndrome: an update. Sao Paulo Med J. 2009 Jul;127(4):223-30. Review.

84. Osada H, Honda N, Takahashi T, Oku S, Abe A, Watanabe W, Okada T, Ohno H, Hondo M, Nishimura K. Relationship between (99m) Tc-GSA scintigraphic indices of liver function reserve and portal circulation in patients with chronic liver disease. Ann Nucl Med. 2007 Jul;21(5):245-9. Epub 2007 Jul 25.

85. Cao X, He N, Sun J, Tan J, Zhang C, Yang J, et al. Hepatic radioembolization with Yttrium-90 glass microspheres for treatment of primary liver cancer. Chin Med J (Engl) 1999;112:430-2.

86. Ajmi S, Hassine H, Guezguez M, Elajmi S, Mrad Dali K, Karmani M, Zayane A, Essabbah H. Isotopic exploration of hepatic hydrothorax: ten cases. Gastroenterol Clin Biol. 2004 May;28(5):462-6.

87. Menzel J, Schober O, Reimer P, Domschke W. Scintigraphic evaluation of hepatic blood flow after intrahepatic portosystemic shunt (TIPS). Eur J Nucl Med. 1997 Jun;24(6):635-41.

88. Richter GM, Brado M, Simon C, Mädler U, Radeleff B, Roeren T, Sauer P, Kauffmann GW. [Changes in liver perfusion caused by transjugular intrahepatic stent shunt (TIPSS)]. [Article in German] Zentralbl Chir. 1997;122(2):108-16.

 2221-0288(201401/01)4:1<01:RLIITA>2.0.TX;2-M